International Research Journal of Engineering and Technology (IRJET) e-ISSN: 2395-0056
Volume: 11 Issue: 05 | May 2024 www.irjet.net p-ISSN: 2395-0072

Numerical Analysis of Aerodynamic Characteristics of Aeroplane Wing with Winglets

Md. Shahadat Hossan Sayem[1], Md. Mainuddin Sagar[2], Md. Rezwan Alam[3], Dr. Abdullah Al-Faruk[4],

[1,3]Research Scholar, Department of Mechanical Engineering, Khulna University of Engineering & Technology, Khulna, Bangladesh
[2]Research Scholar, Department of Mechanical Engineering, Chittagong University of Engineering & Technology, Chittagong, Bangladesh
[4]Professor, Department of Mechanical Engineering, Khulna University of Engineering & Technology, Khulna, Bangladesh

---

Abstract - *This effort examined the potential of winglets on wings in aircraft for the reduction of induced drag coefficient and the increase of lift coefficient without increasing the span of the wings. In this study, the aerodynamic characteristics of an airfoil wing having winglets have been studied with the help of simulation software ANSYS Fluent. Here, the drag co-efficient and lift coefficient have been studied for different cant angles of winglets on aircraft wing. For the effort, subsonic flow of air will be considered over the wing. NACA 0012 symmetric airfoil is considered for the study. In this report, the pre-effort for numerical analysis of the using and performance of winglets have been observed and also, the shape of the wing and winglets. From the study, it is observed that the lift to drag coefficient ratio exhibits maximum values for wing with 90° winglet. The values of CL/CD shows lowest values for normal wing. In the case of wing with 30° and 45° winglet, the values or curves seem similar with each other. Blended winglet will increase lift coefficient about approximately 42% to 49% and reduce drag coefficients. These winglet designs are capable of reducing the induced drag and converting wing tip vortices to increase thrust, saving costs by reducing fuel consumption, reducing noise levels and enhancing aircraft engine performance.*

Key Words*: *NACA, Aerofoil, Winglets, Lift Coefficient, Subsonic Flow, Reynolds Number, Chord Length

1.INTRODUCTION

Wings are the most important and vital part of an aeroplane which keeps the aircraft floated and steady and also helps it to move through a direction into the air stream of surroundings. More than 100 years ago, aircraft designers sought to improve the existing methodologies for aircraft control.. An airfoil-shaped body, called 'Wing' which moves through a fluid produces an aerodynamic strength. The part of this force is called raise which is perpendicular to the direction of motion. The parallel aspect to the direction of free stream motion is called drag. Subsonic flight airfoils have a typical form with a rounded leading edge, accompanied by a straight trailing edge, often with upper and lower surface curvature symmetrical. Foils constructed with water with similar function as the operating fluid are called hydrofoils. A winglet is an almost vertical extension to the tips of the wing. The winglet's upward angle (or Cant), its inward angle (or toe), as well as its size and shape are critical for proper performance, and unique in every application.

Winglets help mitigate the effects of "induced drag." Most airplanes are designed so that the outer tips of the wing are higher than where the wings are attached to the fuselage. This upward angle is called the dihedral and helps to keep the airplane from rolling unexpectedly during flight. When an aircraft is in flight, the air pressure on top of the wing is lower than the air pressure under the wing. That's why there would be a pressure difference between the upper surface of the wing and the lower surface of the wing causing a pressure gradient region. That would result in the desired lift which would help an aircraft to float in the air considering the required consequences. A winglet is a vertical or inclined attachment of the wing tips. Winglets make it easier for the wings to generate lift, which ensures the planes need fewer input from the engines. Winglets has been used extensively as they offer better fuel efficiency for the aircraft.

The winglet transforms some of the otherwise wasted ene rgy into an apparent thrust in the wingtip vortex. This small contribution can be worthwhile, provided the benefit offsets the cost of installing and maintaining the winglets during aircraft's lifetime. The vortex that rotates around from Mow the wing impacts the winglet's cambered surface, creating certain angles with a push. Also they can perform to reduce the strength of the wing tip vortex, which trails downstream of the plane. It is a high risk for an aircraft to pass through these vortices, the turbulent air can push the aircraft into an accident by causing loss of control.

In the 1970s, biologists began to explore the flying characteristics of soaring birds, such as eagles, hawks, condors, vultures and ospreys. Each of these birds has high lift wings at the ends that produce slotted wingtips with feathers called "pin." Biologists find that the pin feathers function in the same manner as aircraft ailerons in reducing drag while gliding as well as in roll control. As for the California Condor, these multi-winglets are quite often long and prominent. . He used small, nearly vertical fins installed on a KC-135A and flight tested1-2 in 1979 and 1980. The winglet concept actually dates back to patent in 1897, but not until Whitcomb investigated winglet aerodynamics did the concept mature. Whitcomb found that at cruising speeds, winglets could increase the range of an aircraft by as much as seven per cent. A NASA contract3 in the 1980s assessed winglets and other drag reduction devices, and they found that wingtip devices (winglets, feathers, sails, etc.) can improve drag-due-to-lift efficiency by 10 to 15% if they are designed as an integral part of the wing. Several types of improvements to the wingtip have been patented in recent years. The tip6 "spiroid" wing creates a decrease in the induced drag, comparable to that of a winglet. Although the wing tips may be eliminated by a closed lifting system, this does not eliminate the trailing vortex wake. By eliminating the discontinuity between the wing tip and the winglet, the blended winglet10 reduces drag. A smoothed version is being used on the Boeing 737-400's gently upswept winglet. Boeing Business Jets and Aviation Partners, Inc. have embarked on a cooperative program to market the Boeing 7xx series of jetliners with conventional winglets for retrofit.

2. LITERATURE REVIEW

In those early years, structural compliance techniques were actively incorporated into aircraft structures as a means of controlling aircraft with the most notable technique being the ingenious "wing warping" used for roll control by the Wright brothers **Error! Reference source not found.**. The last 25 years have spanned modern interest in winglets. NASA Langley Research Center's Richard Whitcomb **Error! Reference source not found.** first looked at modern winglet applications for aircraft transport in the 1970's. Bourdin et al.**Error! Reference source not found.**, investigated a novel method for the control of “Morphing” aircraft. At that concept, a pair of winglets are consisted with adjustable cant angle, attached at the tips of a baseline flying wing and actuated independently. A vortex lattice model is computed and subsequent wind tunnel tests are demonstrated the viability of the concept. Comparisons are made to good agreement between the experimental and numerical findings, with the main differences assumed to be attributed to aeroelastic effects of the wind tunnel model.

Houghton **Error! Reference source not found.** observed that if a winglet is attached to a wing then it would substantially reduce the flutter speed of the wing in transonic Mach number. Therefore, the result of slide slips on winglets is to produce increased loads similar to wing loads due to angle of attack. Satran demonstrated the static and dynamic stability and control and free-flight behavior of a 0.36 scale model of a canard general-aviation airplane with a single pusher propeller and winglets in the Langley 30 by 60 feet wind tunnel. He consider the model showing very strong dihedral impact but poor steering stability. Analysis and design of wings and wing/winglet Combinations at low speeds is done by Chattot **Error! Reference source not found.** who considered numerical treatment in Prandtl lifting –line theory of the non-linearity associated with a 2-D lift curve, when the local incidence is greater than the incidence of maximum lift. An artificial viscosity term has been acquainted to the governing equation that allows the iterative method to converge to the correct solution. The effect of yaw has been determined and the optimal wing/winglet combinations have been found to have weathercock stability.

Gall et al. **Error! Reference source not found.** examined both theoretically and experimentally, the most likely improving the aerodynamic characteristics of a biplane configuration by adding winglets. A good agreement with experiment in predicting inviscid drag due to lift is exhibited by theoretical calculations. The ideal efficiency factor is increased up to 13% as well as increasing the lift curve slope and maximum lift coefficient. A statistical study compared the biplane with an improve d winglet to a monoplane reveals the biplane has the pote ntial to increase L / Dmax by 6.4 per cent and 13 percent increase in CL 3/2 / CD , the classical endurance parameter. Research by evolutionary biologists at the Technical University of Berlin has also shown the effectiveness of several slotted wings and shown how these traits could have evolved naturally in birds by gradually increasing wing performance. Their evolutionary theory has been emulated in an aircraft optimization algorithm developed by Kroo et al. **Error! Reference source not found.**, which has discovered a ‘C’-wing configuration with a winglet and a horizontal extension that shows reduced drag for fixed lift, span, and height.

Kroo et al. **Error! Reference source not found.** dealt with the broad concept of non-planar wings, which includes winglets. They examined a variety of aircraft types, including winglets, nag wings, box wings and the exploitation of non-planar wakes in general. Such designs are of interest because of their potential for lower vortex drag without increased span, a key constraint for many aircraft. The Wright brothers exploited the structural advantages of biplanes. At very low Reynolds number,

highly cambered, thin sections, making the cable braced Wright biplane concepts especially attractive. However, Smith et al.**Error! Reference source not found.** figured out that the adjustments of single winglets onto the biplanes improves 13% in endurance, as well as increasing the lift-curve slope and the maximum lift coefficient of the vehicle. Jonathan Santos anticipated the innovation in the current proposal in his patent on wingtip airfoils. Santos realized that a sequence of winglets at the wingtips could take advantage of the spiral design of the wingtip vortices to increase a single winglet's efficiency. At the Cranfield Institute of Technology in England, Spillman et al.**Error! Reference source not found.** carried out a series of programs to investigate devices akin to the wing tip airfoils, which he called "wing tip sails". He explored the use of one to four sails on a Paris MS 760 Trainer aircraft wingtip fuel tank. Flight test experiments confirmed the wind tunnel tests, and demonstrated shorter takeoff rolls and reduced fuel consumption. Spillman later determined wingtip vortex reduction due to wing tip sails, and found lower vortex energy 400-700 m behind the aircraft, although the rate of decay beyond that was somewhat lower.

Hossain et al.**Error! Reference source not found.** investigated about the aerodynamic characteristics for aircraft wing model with and without bird feather like winglet. NACA 653-218 airfoil is used in this regard. The experimental analysis shows that a decrease of 25-30 percent in the drag coefficient and a 10-20 percent increase in the lift coefficient by using bird feather like winglet for angle of attack 8 degrees. Beechook et al. **Error! Reference source not found.** found that the efficiency of an aircraft is greatly affected by induced drag generated by wingtip vortices. Winglets at aircraft wingtips, referred to as vertical or angled extensions, are used to reduce the creation of vortices to increase the fuel efficiency.

The objectives of the study were to analyze the aerodynamic characteristics and to examine winglet efficiency at cant angles 0 °, 30 °, 45 °, and 60 ° at different angles of attack (AOA). The experimental work was carried out under conditions at sea level and free-stream velocity of 35 m / s in a closed-loop wind tunnel. Using Finite Volume Process, the CFD simulations were performed at low subsonic flow rate in ANSYS CFX solver. Cosin et al.**Error! Reference source not found.** developed a multi-winglet study as a method for minimizing induced drag in low-speed aircraft, based on experimental observations of the Re= 4x105 wing-body semi-model. A baseline and six other configurations of different multi winglets were tested. The system resulted in a gain of 32 per cent in the Oswald performance metric, reflecting a 7 per cent increase in the overall aerodynamic efficiency. Improvements were also made in the overall climb average of 12 per cent and in the maximum range of 7 per cent. The pressure distribution was tested to validate multi-winglet global and local impacts, showing only a small impact of the unit on the wing filling. Also conducted were structural investigations as well as wake-up surveys using a seven-hole Pitot probe which revealed significant changes in the flow field near the wingtip.

Mattos et al.**Error! Reference source not found.** discussed some of the experience acquired in modeling winglets for several aircraft types, varying from a business jet and a 70-passenger twinjet airliner to an AEW&C military aircraft. Embraer's experience and the widespread use of winglets in new aircraft designs allow us to conclude that the old question about the feasibility of designers adopting winglets is no longer valid. Instead a new issue is currently in place about the option of the best configuration of the wingtip unit. Pfeiffer et al. **Error! Reference source not found.** introduced a procedure for maximizing a winglet's orientation on a wing and included the results of profile drag as well as the caused drag. The method makes use of the performance from four potential-flow solutions well behind the lifting surfaces in the Trefftz plane. The four alternatives are a reference, an improvement in angle of attack, an increase in the winglet's root incidence, and an increase in the winglet's tip incidence. Results for the case studied show small differences in the incidences of root and tip between an induced-drag-only solution and one which includes profile drag. Himisch **Error! Reference source not found.** investigated to demonstrate a tool for estimating the aerodynamic effect of a design shift in a local wall. A winglet was created for a specific configuration in the illustration described. To choose the most promising design, a lifting line approach was used to reduce the amount of computation time taking into account the specified structural boundary conditions. Since lifting line methods are only capable of predicting the induced drag effect, initial numerical simulations of the base reference geometry were used to understand some of the additional effects, such as that of increasing the wetted surface area by contrasting those numerical findings with the established equations of a quadratic polar drag.

Myilsamy et al.**Error! Reference source not found.** found that winglet wing generates higher performance in the Cl / Cd ratio than standard wingletless aircraft. His performance has been diminished up to a certain degree of angle of attack and by increasing further to a higher angle of attack. The concept of variable angle winglets under investigation appears to be a promising alternative for improving an aircraft's aerodynamic efficiency.

3. DESCRIPTION AND DESIGN

3.1 Theoretical Description:

Aerodynamics is an applied science which deals with the movement of air or something that moves in the air. It is generally used for problem arising from flight and other

topics involving with the flow of air. Aerodynamic forces and moments on the body takes place due to two reasons – 1. Pressure distribution over the body surface and 2. Shear stress distribution over the body surface. Pressure acts normal to the surface and shear acts tangential to the body surface. Shear stress due to "tugging action" on the surface, which is caused by the friction between body and the air. The net effect of the pressure distributions and the shear stress distribution integrated over the complete body surface is a resultant force and moment acting on the body. Lift and drag are the two components of this resultant force.

If the flight speed is small compared with the speed of sound, the changes in pressure which are generated by the vehicle motion are small relative to the free-stream static pressure, and the influence of compressibility can be neglected. Hence, the flow can be assumed as incompressible. Streamlines converge as the incompressible flow accelerates past the midsection of an airfoil. The widening of the stream tubes near the nose and the contraction of the stream tubes in the regions of increased velocity lead to a progressive reduction in the curvature of the streamlines. As a consequence, the flow distortion is easily attenuated by distance from the airfoil. In this study, the flow is considered as an incompressible where the density of flow does not vary with time in a flow field.

The varieties of air flowing over the body surface can be classified into several types such as 1. Subsonic flow 2. Supersonic flow 3. Transonic flow 4. Hyper-sonic flow. In this study, subsonic flow over the wing surface is considered for low flight speeds where the Mach number (the ratio of free stream velocity to standard air velocity) is less than unity. Subsonic flow are characterized by smooth streamlines (no discontinuity in slope).

Mach number less than 1 does not guarantee a totally subsonic flow over the body. In expanding over an aerodynamic shape, the flow velocity increases above the free-stream value (V∞) and if M∞ is close enough to 1, then the local Mach number may become supersonic in certain regions of the flow. It gives rise to a thumb law that for subsonic flow over slender limbs, M denotes < 0.8.

Lift is mainly due to the imbalance of pressure distributions between the upper body surface and lower body surface of the aerodynamic shape. Specially, the pressure of aerodynamic shape is lower on top surface than lower surface which results in lifting of the object. Aerodynamic flow over the airfoil or wing follows the law of nature- continuity equation and momentum equation or Newton's Second law. Because of the Bernoulli's effect, the flow velocity over the aerodynamic shape increases when the static pressure decreases on the top body surface. On the contrary, the flow velocity decreases on the bottom body surface as the static pressure increases satisfying the Bernoulli's theorem **Error! Reference source not found.**.

The lift coefficient (CL) is a dimensionless coefficient that relates the lift generated by a lifting body to the fluid density around the body, the fluid velocity and an associated reference area. A lifting body is a foil or a complete foil-bearing body such as a fixed-wing aircraft. CL is a function of the angle of the body to the flow, its Reynolds number and its' Mach number. The lift coefficient cl refers to the dynamic lift characteristics of a two-dimensional foil section, with the reference area replaced by the foil chord.

Drag coefficient (CD) is a dimensionless quantity that is used to quantify the drag or resistance of an object in a fluid environment, such as air or water. It is used in the drag equation in which a lower drag coefficient indicates the object will have less aerodynamic or hydrodynamic drag.

Lift Coefficient and drag coefficient are defined as,

$$C_L = \frac{L}{\frac{1}{2}*\rho_\infty*{V_\infty}^2} \quad \text{..... (3.1)}$$

$$C_D = \frac{D}{\frac{1}{2}*\rho_\infty*{V_\infty}^2} \quad \text{..... (3.2)}$$

Where,

L is the lift force in N, and D is the drag force in N, ρ_∞ is the density of air in kg/m3, V_∞ is the free stream velocity of air in m/s, c is the chord length in m, S is reference area in m2. Using equations of state for perfect gas the air density, ρ_∞ kg/m3 is defined as,

$$\rho_\infty = \frac{P}{RT} \quad \text{..... (3.3)}$$

Where, P is the absolute pressure in N/m2, T is the temperature in K and R is the gas constant of air in Nm/(kg) (K). Reynolds number is used to indicate whether a fluid flowing around or through a body is laminar or turbulent. It is the ratio of the inertia force to the viscous force of a fluid flowing around some boundary. Based on the chord length of an airfoil, Reynolds number is defined as,

$$Re_\infty = \frac{\rho_\infty \times V_\infty \times c}{\mu_\infty} \quad \text{..... (3.4)}$$

Where, V_∞ is the free stream velocity in m/s; μ_∞ is the dynamic viscosity in kg/(m)(s) and c is the chord length in m. The air viscosity μ_∞ is determined using the Sutherland's equation described below,

$$\mu_\infty = 1.458 \times 10^{-6} \times \left(\frac{T^{1.5}}{T+110.6}\right) \quad \text{..... (3.5)}$$

Where, T is the temperature in K.

However, in all real aeroplane wings, the flow over the wing is 3 dimensional flow having a component a span wise direction. Since incompressible flow passes pressure information in all direction equally, pressure variation can be sensed between the upper surface and lower surface of the wing. Due to the pressure imbalance around the wing, the flow at the wingtip tends to curl around the tip (leak or spill out around the wingtip) from the high pressure region just underneath of the wing to the low pressure region on top.
As a consequence of spill out of flow tendency around the wingtip equalizes the pressure between the bottom and top surface of the wing. This causes lift force per unit span decreases towards the wingtip. As a result of the span wise pressure variation, the air on the upper surface flows inboards toward the root. Similarly, on the lower surface, air will tend to flow outward toward the tips. The resultant flow around the wing is 3 dimensional having both chord wise and span wise velocity components.

When the flows from the upper surface and lower surface join at the trailing edge, the difference in span wise velocity components causes the air to roll up into a number of cortices at the wingtips. These small vortices roll up into two large vortices just in board of the wingtips called the tip vortex. Since the lift force acting on the wing section at a given span wise location is related to the strength of circulation, such that the circulation around the wingtip is zero.

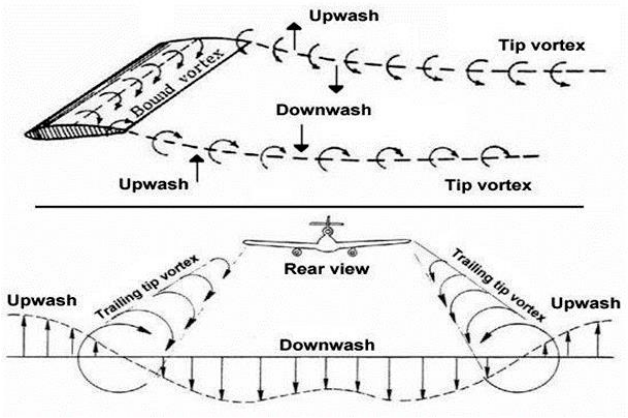

Fig. 1: The Development of Wingtip Vortices **Error! Reference source not found.**

3.2 Airfoil Description and Design:

An airfoil is the cross sectional shape of a wing or wing turbine blade or a sail used in propeller, motor blade etc. The NACA airfoil sections considered herein are obtained by combining a thickness distribution and a mean line. An airfoil is obtained from a perpendicular plane with respect to the corresponding wing considered as a cross section shape.

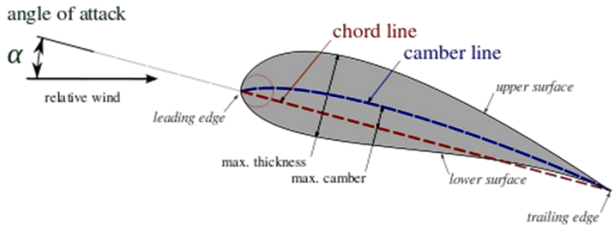

Fig. 2: A typical airfoil with corresponding terms **Error! Reference source not found.**

Some terms are related to the description of the airfoil. The major design feature of an airfoil is the mean line, which is the locus of points halfway between the upper and lower surfaces as measured perpendicular to the mean line itself. The most forward point of a mean line is known as the leading edge and the most rearward point of the mean line is known as the trailing edge. A straight line which connects between the leading edge and trailing edge is known as chord line of the airfoil and the distance measured simply between the leading edge and trailing edge is known as chord of the airfoil, which is designated by 'c'. The Camber is considered as the maximum distance between the mean camber line and the chord line, measured perpendicular to the chord line. Two basic types of airfoil can be demonstrated or used extensively which are, symmetrical airfoil and non-symmetrical airfoils. Symmetrical airfoils used to have no camber in itself as the mean camber line and the chord line is same in this case. On the contrary, non-symmetrical airfoils are also known as cambered airfoils. Cambered airfoils shows lifting characteristics even at 0 degree angle of attack (angle between the free-stream velocity and the chord line of the airfoil) due to its cambered type shape. But in the case of symmetrical of non-cambered airfoil, there would no lift at 0 degree angle of attack due to symmetrical shape of the airfoil. The camber, the shape of the mean camber line and to a lesser extent, the thickness distribution of the airfoil essentially controls the lift and moment characteristics.

There are several types of NACA airfoils families used as cross section shape in construction of wing of airplane. For example, NACA 4 digit series, NACA 5 digit series and NACA 6 digit series. In this study, NACA 4 digit series is considered. The first digit of the designated number indicates the locus of the maximum positional point of the corresponding airfoil in number of hundreds of the chord of the airfoil. The second digit indicates the horizontal distance of the maximum camber from the leading edge of the airfoil in number of tenths of the chord of the airfoil. And the last two digits indicates the maximum thickness of the airfoil in hundreds of the chord of the airfoil.

If Xu and Yu represent respectively the abscissa and ordinate of a typical point of the upper surface of the airfoil and yt is the ordinate of the symmetrical thickness

distribution at chord wise position Xi, the upper surface coordinates are given by the following relations:
Yu = yt

The corresponding expressions for the lower surface coordinates are:
Xt = x
Yt = -yt

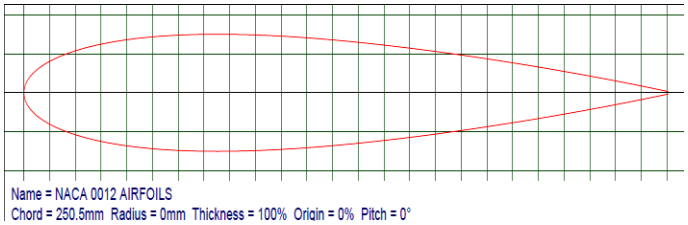

Fig. 3: Designed NACA 0012 airfoil [14]

3.3 Description of NACA 0012 Airfoil:

NACA 0012 is a symmetrical airfoil meaning that it has zero camber in its symmetrical shape. The 2 digits '00' indicates that it is a symmetrical airfoil and the last 2 digit '12' indicates that the maximum thickness of the airfoil is 12% of the chord length of the airfoil.

The equation for a symmetrical 4-digit series NACA airfoil is

$$y_t = 5t\left[0.2969\sqrt{\frac{x}{c}} - 0.1260\left(\frac{x}{c}\right) - 0.3516\left(\frac{x}{c}\right)^2 + 0.2843\left(\frac{x}{c}\right)^3 - 0.1015\left(\frac{x}{c}\right)^4\right]$$

…….. (3.6)

Where,

x is the position along the chord from 0 to c

t is the maximum thickness as a fraction of the chord

c is the chord length

The leading edge is constructed as a part of cylindrical shape with a radius of
r = 1.1019 t2

Now the coordinates (Xu, Yu) of the upper airfoil surface, and (Xu, Yl) of the lower airfoil surface are:

Xu = Xl = x
Yu = + y and
Yl = - yt

Table 1 : Airfoil specifications at different sections for geometry designing

Serial No.	Parameter	Chord length, C (mm)	Thickness, t (mm)	Trailing edge radius, r (mm)	Camber (mm)
01	Wing root	250.5	30.06	995.68	0
02	Wing tip	85.81	10.2971	116.834	0
03	Winglet root	85.81	10.2971	116.834	0
04	Winglet tip	45	5.4	32.1314	0

3.4 Governing Equations for CFD Analysis:

Continuity equation, Navier Stokes or Momentum equation and Energy equation are the key governing equation of the fluid dynamics which are also instrumental for Computational Fluid Dynamics (CFD). From simple creeping flow, and Couette flow, to the state-of-the-art turbulence modelling, moving boundaries simulation, nanofluids motion, multiphase flow, complex geometry aerodynamic design wave modelling and oceanic engineering, all these engineering researches fall under the purview of these governing equation. The governing equations stem from the fundamental principles of Newton's Laws and Reynold's transport theorem, which can be expressed in a general form of integral equations. In this aerodynamic study, energy equation is not considered for basic purpose.

3.4.1 Continuity Equation:

The fundamental physics of Continuity Equations is the principle of conservation of mass, proposed by Lavoisier in 1985. Conservation of mass can be defined as: the conservation law that the rate of change of mass within a control volume (CV) is equivalent to the net rate of mass flowing into the CV. Consider the integral form of the mass conservation equation:

$$\frac{\partial}{\partial t}\int_{CV}\rho.dV + \int_{CS}\rho.\boldsymbol{V}.\bar{\boldsymbol{\eta}}.dA = 0$$ …….. (3.7)

This equation can be transformed into differential form using Gauss Divergence theorem to form

$$\dot{\rho} + \nabla(\rho\boldsymbol{V}) = 0$$ ……. (3.8)

In Cartesian co-ordinate, considering the length of fluid element infinitesimal in x, y and z direction, can be assigned as δx, δy and δz. Taking, V= [ux uy uz] in an incompressible flow, the continuity equation will be reduced to where

$$\nabla.\mathbf{V} = \mathbf{0}$$

$$\nabla = \frac{\partial}{\partial x} + \frac{\partial}{\partial y} + \frac{\partial}{\partial z}$$

3.4.2 Navier Stokes Equation or Momentum Equation:

Momentum equations are originated from Newton's second law which states that force of a moving object is equivalent to its rate of change of momentum.

$$\frac{\partial(\rho u)}{\partial t}+\frac{\partial(\rho u^2)}{\partial x}+\frac{\partial(\rho uv)}{\partial y}+\frac{\partial(\rho uw)}{\partial z}=-\frac{\partial p}{\partial x}+\frac{\partial}{\partial x}\left(\lambda\nabla.\boldsymbol{V}+2\mu\frac{\partial u}{\partial x}\right)+\frac{\partial}{\partial y}\left[\mu\left(\frac{\partial v}{\partial x}+\frac{\partial u}{\partial y}\right)\right]+\frac{\partial}{\partial z}\left[\mu\left(\frac{\partial u}{\partial z}+\frac{\partial w}{\partial x}\right)\right]+\rho f_x$$

…….. (3.9)

$$\frac{\partial(\rho v)}{\partial t}+\frac{\partial(\rho uv)}{\partial x}+\frac{\partial(\rho v^2)}{\partial y}+\frac{\partial(\rho vw)}{\partial z}=-\frac{\partial p}{\partial y}+\frac{\partial}{\partial x}\left[\mu\left(\frac{\partial v}{\partial x}+\frac{\partial u}{\partial y}\right)\right]+\frac{\partial}{\partial y}\left(\lambda\nabla.\boldsymbol{V}+2\mu\frac{\partial v}{\partial y}\right)+\frac{\partial}{\partial z}\left[\mu\left(\frac{\partial w}{\partial y}+\frac{\partial v}{\partial z}\right)\right]+\rho f_y$$

…….. (3.10)

$$\frac{\partial(\rho w)}{\partial t}+\frac{\partial(\rho uw)}{\partial x}+\frac{\partial(\rho vw)}{\partial y}+\frac{\partial(\rho w^2)}{\partial z}=-\frac{\partial p}{\partial z}+\frac{\partial}{\partial x}\left[\mu\left(\frac{\partial u}{\partial z}+\frac{\partial w}{\partial x}\right)\right]+\frac{\partial}{\partial y}\left[\mu\left(\frac{\partial w}{\partial y}+\frac{\partial v}{\partial z}\right)\right]+\frac{\partial}{\partial z}\left(\lambda\nabla.\boldsymbol{V}+2\mu\frac{\partial w}{\partial z}\right)+\rho f_z$$

…….. (3.11)

3.5 Wing Model Designing:

The CAD model of normal wing and wing with winglet are designed by using Solid Works 2016 software. The airfoil data for NACA 0012 [15] is imported to the Solid Works software and the sketch for the airfoil is generated for wing root and also for wingtip. The span length of the wings is considered 500 mm. The maximum and minimum chord lengths for the wing are 250.50 mm and 85.81 mm respectively. Thus the chord length based Reynolds number relevant at low flight speed or subsonic speeds. The chord length of the model was determined to have Reynolds number of the same order. The span length of the model, relative to the chord length is one of the important design parameters.

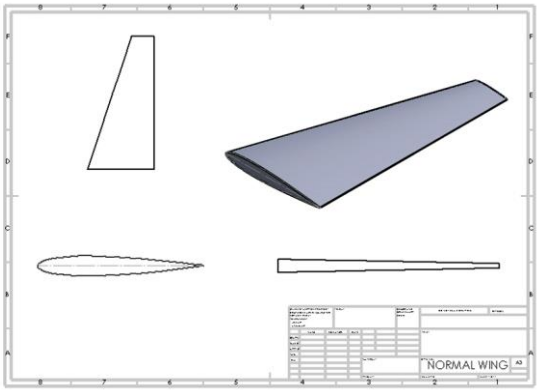

Fig. 4 Designed aircraft normal wing model with no winglet

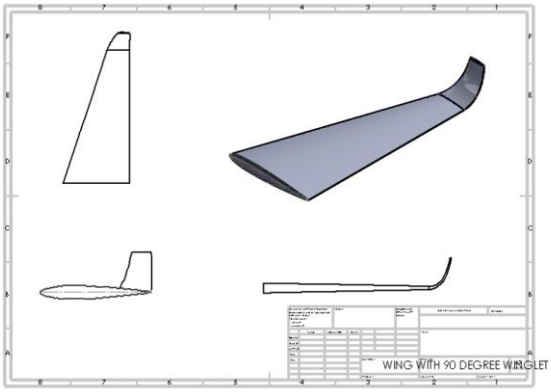

Fig. 4: Designed aircraft wing model with 90 degree winglet

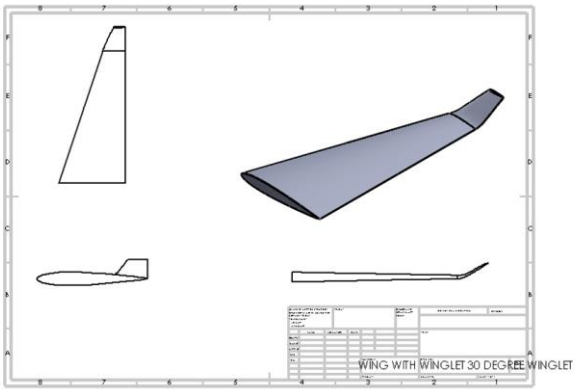

Fig. 5: Designed aircraft wing model with 30 degree winglet

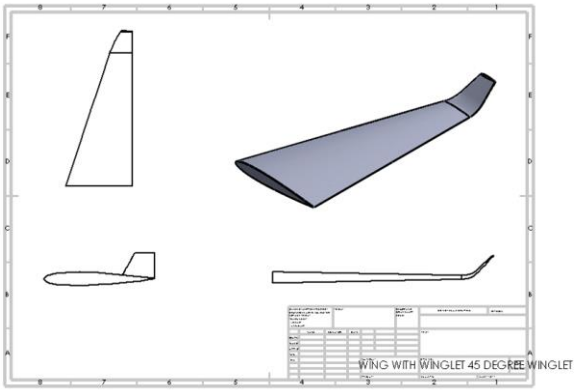

Fig. 6: Designed aircraft wing model with 45 degree winglet

Table 2: Specifications of Aircraft Wing

Serial No.	Description	Dimension
01	Airfoil Type	NACA 0012
02	Wing Type	Swept Back
Spev03	Sweep Angle	18.23 degree
04	Wing Span	500 mm
05	Taper Ratio	0.342
06	Aspect Ratio	2.92
07	Wing Area	0.17104 m2
08	Maximum Chord	250.50 mm
09	Minimum Chord	85.81 mm

Table 3: Specifications of Winglets

Serial No.	Description	Dimension
01	Winglet type	Blended Winglet
02	Winglet Height (30°,45° & 90°)	42.88 mm, 57.18 mm & 90mm
03	Winglet Taper Ratio	0.5244
04	Maximum Chord	85.81 mm
05	Minimum Chord	45 mm

4. METHODOLOGY

4.1 Proposed Methodology:

Computational Fluid Dynamics (CFD) process is used for assisting the numerical analysis of this study. The numerical analysis usually consists of 3 stages: pre-processing, computation and post-processing. The pre-processing stage involves with the geometry generation and setup and grid (mesh) generation. The computational domain (C-domain) is constructed as fluid properties around the 3-D geometry followed by the mesh generation using ANSYS Workbench R19.2 software. The mesh element size is smaller close to the wing and winglet geometry and gradually increases towards the domain boundary walls. 3-D unstructured tetrahedral mesh with inflation layers was generated around the geometry. This was carried out in order to select an appropriate range for the number of elements in the mesh. Mesh dependency is carried out to ensure the independency of results from the number of elements for the numerical analysis of both normal wing and wing with winglets. In this particular case, the number of mesh elements is considered about 4.2 to 4.9 million numbers of mesh elements for better accuracy of results.

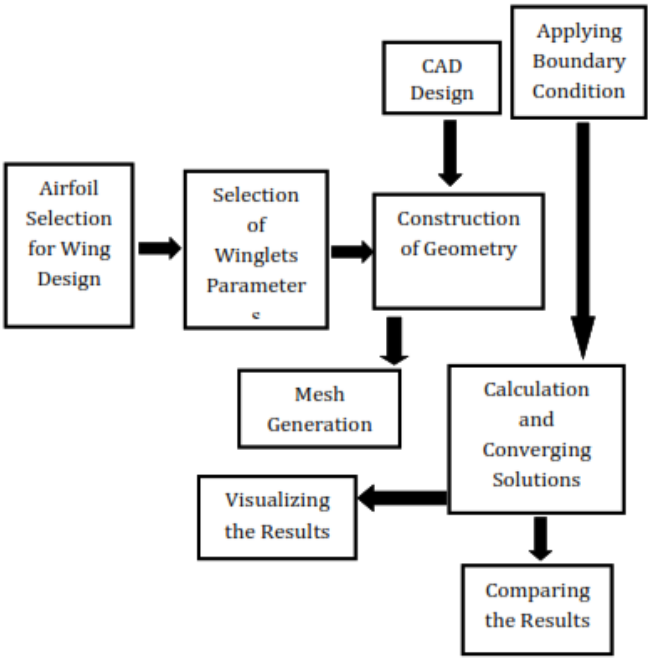

Fig. 8: Flowchart of Proposed Methodology of the study

4.1.1 Geometry Setup:

The designed wing geometry and wing with winglet geometry constructed in Solid works software are exported to the workspace of Design Modeler of Ansys Workbench for further pre-processing works. A C-domain

is constructed for both types of geometry which is assigned as fluid and the previously designed geometries are assigned as solid object. The total volume of the domain around the normal wing geometry is measured about 4.5226 m3 and for the wing with winglet geometry, it is measured about 17.401 m^3

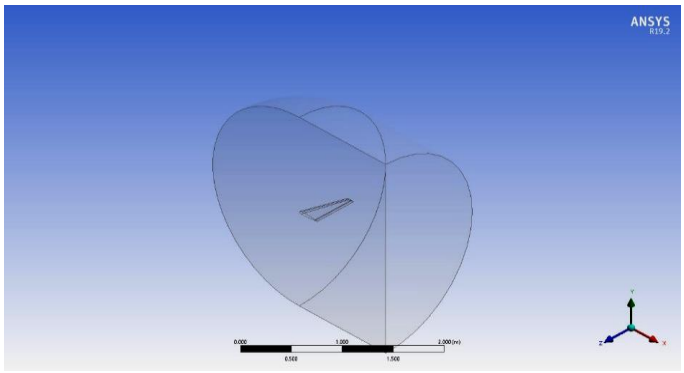

Fig. 9: Geometry setup for numerical analysis of normal wing

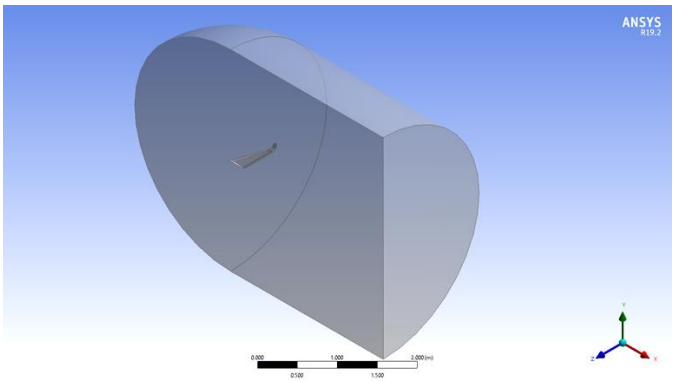

Fig. 10: Geometry setup for numerical analysis of wing with winglet

4.1.2 Mesh Generation:

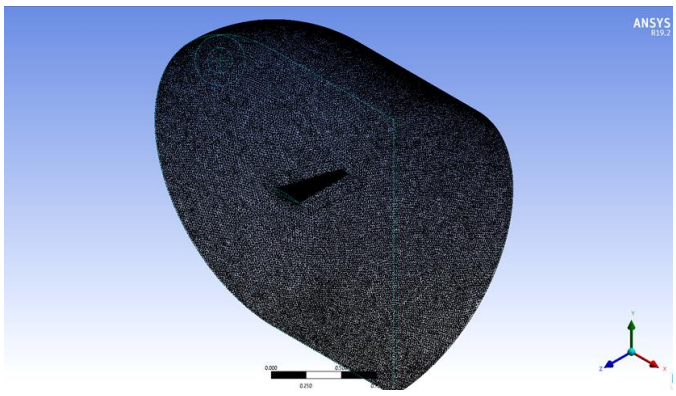

Fig. 11: Mesh generation for normal wing

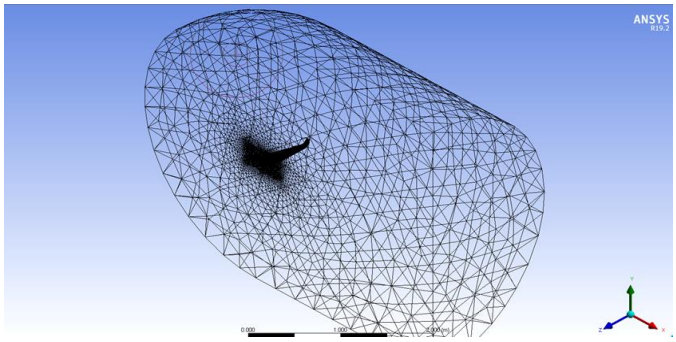

Fig. 12: Mesh generation for wing with winglet

In mesh setup, unstructured tetrahedral mesh elements is assigned for the mesh generation. Body sizing mesh control is done for fluid domain geometry where the solid wing surface is considered as the body of influence. Different mesh element size is done for ensuring the mesh independency on results. Face sizing mesh control is done for meshing the forward and rearward face of the wing surface and also the inward top and bottom of the surface. High quality smoothing is considered for mesh generation. Usually the element size will increase gradually moving forward to the fluid domain and the mesh elements will be smaller so much than the body geometry mesh elements. Inflation is done about considering 5 layers with 0.008 m total thickness. In this case, post inflation algorithm is used. Then, the necessary surfaces are named due to assign the boundary conditions to the fluid domain and wing geometry. In this, inlet, outlet, symmetry, wing surface and wingtip (for normal wing) and wing surface with winglet (for winglets) are named to observe the properties in further post-processing.

4.1.3 Setup:

In the "SETUP" portion of the analysis, the double precision option is checked before starting the configuration of the required setup. In the general settings of the analysis, the solver type is set to pressure based system and the flow type is considered as steady flow. In the models segment, the "multi-phase" option is turned off as the incompressible flow surrounding the airplane wing is being considered. As the study is to found the aerodynamics characteristics of the airplane wing only according to the relative flow properties of air surrounding the wing and winglets, so the energy option is unchecked which is related to the calculation of energy equations. At the viscous model segment, the "k-epsilon" model with standard type is being considered and at "Near Wall Treatment", Standard wall functions are considered as this combination has produced the desired results related to the analysis purposes. The fluid is considered as air and the solid part is considered as aluminum with standard properties. At the boundary conditions segment, the values of flow velocity are inserted for different values of angle of attack at "Inlet" surface as it was defined as the entrance of free stream flow towards the wing geometry at

the +X direction at mesh segment. In this case, at the "Velocity Specification Method" option, the "Magnitude and Direction" option is selected which enable us to specify the X,Y components of the flow direction individually which actually would results in drag forces and lift forces values acting on the wings after completing the numerical calculation. These values has been changed with respect to the change in the values of angle of attack. That is why, a "Parameter" setup is introduced for changing the values of X and Y components of the free stream velocity while changing the corresponding value of angle of attack for a specific wing geometry. This process is repeated for the normal wing geometry, wing with 90º winglet, 45º winglet and 30º winglet geometry respectively. And the outlet is defined as "Pressure Outlet" while setting the back flow turbulent intensity to 5% and the back flow turbulent viscosity ratio to 10. The reference values are computed from the inlet. In monitors segment, two different individual new monitors are created manually to observe the change of values for lift co-efficient and drag co-efficient with respect to the iteration number while doing the numerical calculation. In "Solution Initialization" part, "Standard Initialization" is selected as we would like to solve the calculation from the corresponding inlet values which are defined as boundary conditions at inlet. In the end, the number of iteration are set from 100 up to 10000 for calculation in several different cases. The results are extracted each time after the processed solution is being converged.

Table 4: Boundary Conditions and simulation settings

SI No.	Factors	Considerations
01	Fluid	Ideal Gas
02	Flow Condition	Steady State
03	Inlet	Velocity inlet = 100 m/s (Subsonic Flow)
04	Angle of attack	2-20 degree (as necessary)
05	Outflow	Pressure Outflow
06	Fairfield	Wall
07	Top and Bottom Wall	Wall (No Slip Condition)
08	Convergence Factor	0.001
09	Solver	Pressure Based
10	Viscous Model	k-epsilon (2 equations)

5. RESULTS & DISCUSSION

In this study, the outward flow simulation over 3 dimensional wing will be analyzed. As the free stream air will strike the wing at a specified angle of attack, it is desired to generate lift and drag forces on the surfaces of the wing. The pressure differences between the upper and lower surfaces of the wing will be observed and it would be discussed whether the properties and the regarding acting forces changes with changing flow direction with same type of flow and at a same Reynolds number. After that, the pressure coefficient curves along with the positional line as well as the chord line will be studied whether how differences it would exhibit at different flow directions. Due to considering low Mach number, the flow will be attached at most of the cases of the flow directions. After the stall of airfoils takes place where the maximum lift coefficient is found, the flow separation of the flow may occur.

The pressure contours are shown at "ANSYS Fluent Result" to observe the pressure distribution and changes of it along the chordwise direction as well as spanwise direction. Also a velocity streamline contour is also drawn for showing the direction and observation of streamlines of flow around the wing for both non-winglet and winglet type. The flow streamlines are expected to be at changed direction for each value of angle of attack.

5.1 Pressure and Velocity Streamline Contours for Normal Wing:

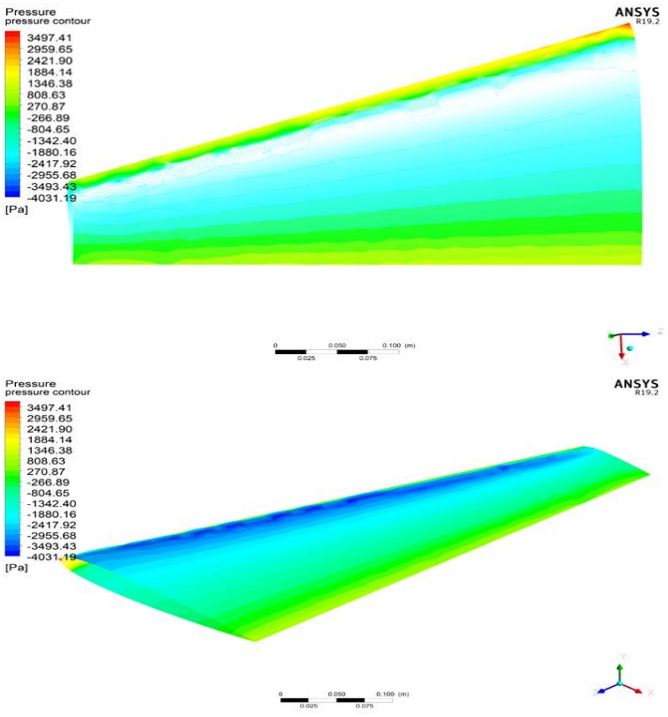

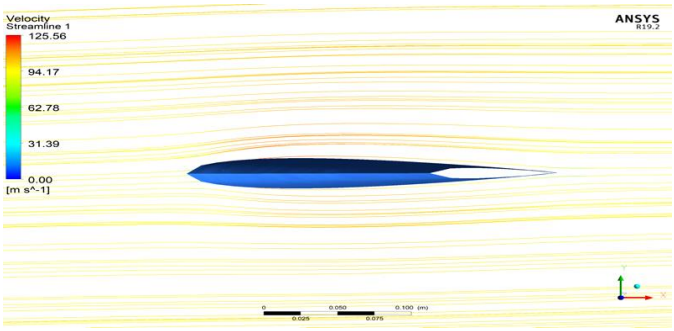

Fig. 13: Pressure distribution and velocity streamline contours for 2° angle of attack

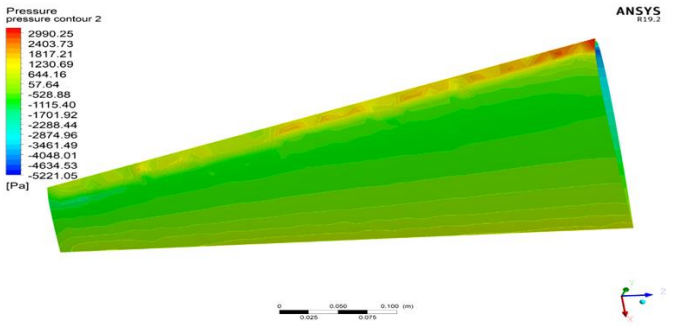

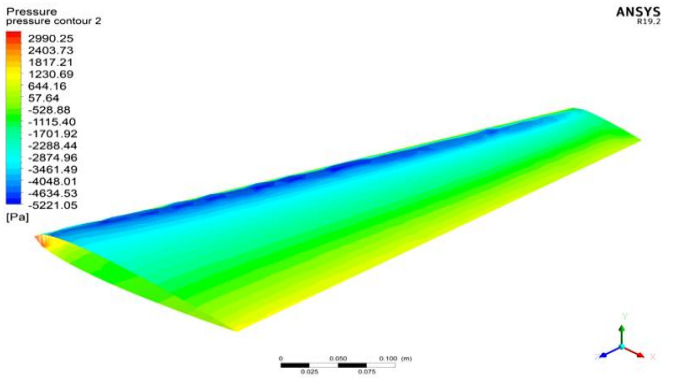

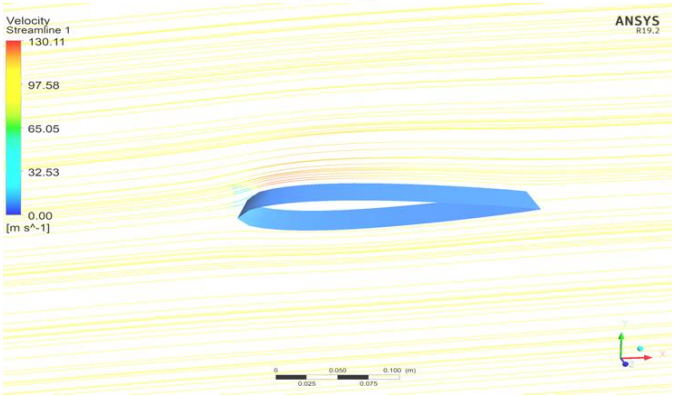

Fig. 14: Pressure distribution and velocity streamline contours for 4° angle of attack

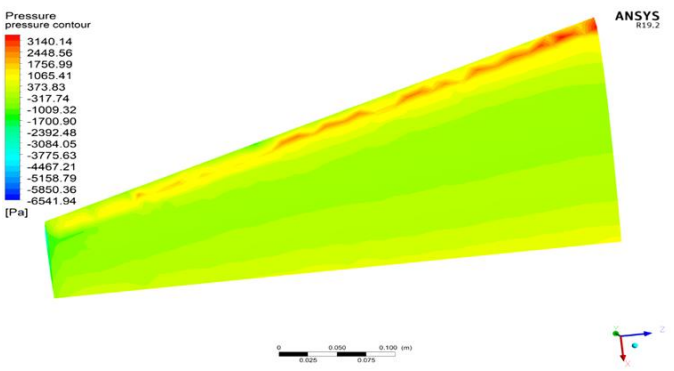

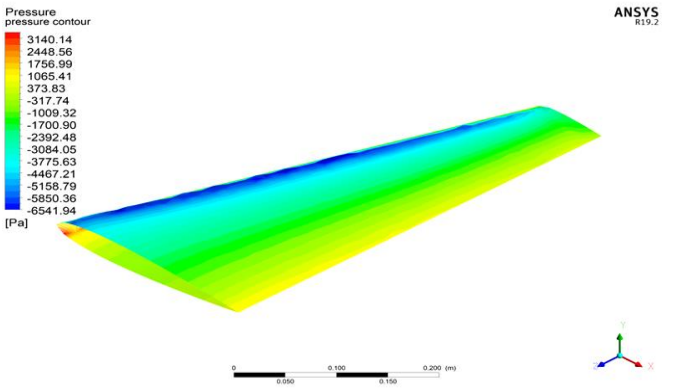

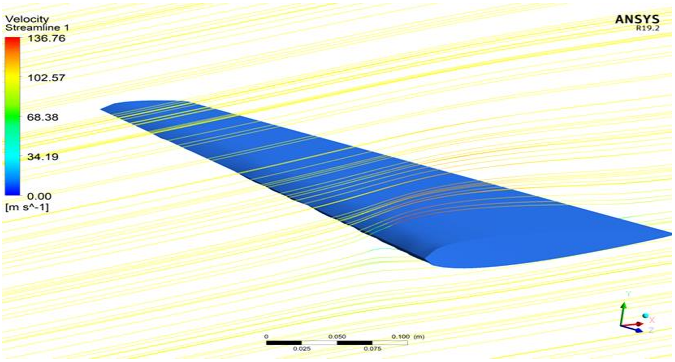

Fig. 15: Pressure distribution and velocity streamline contours for 6° angle of attack

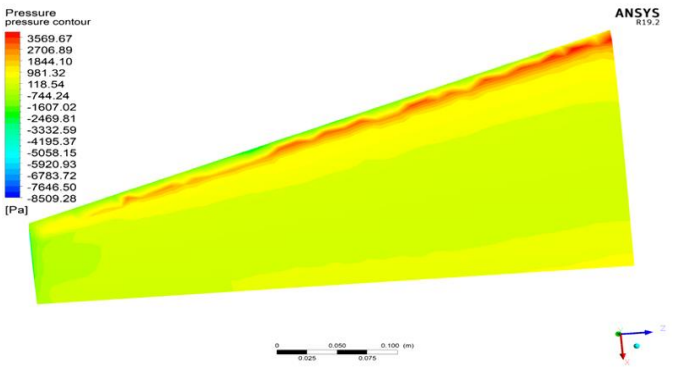

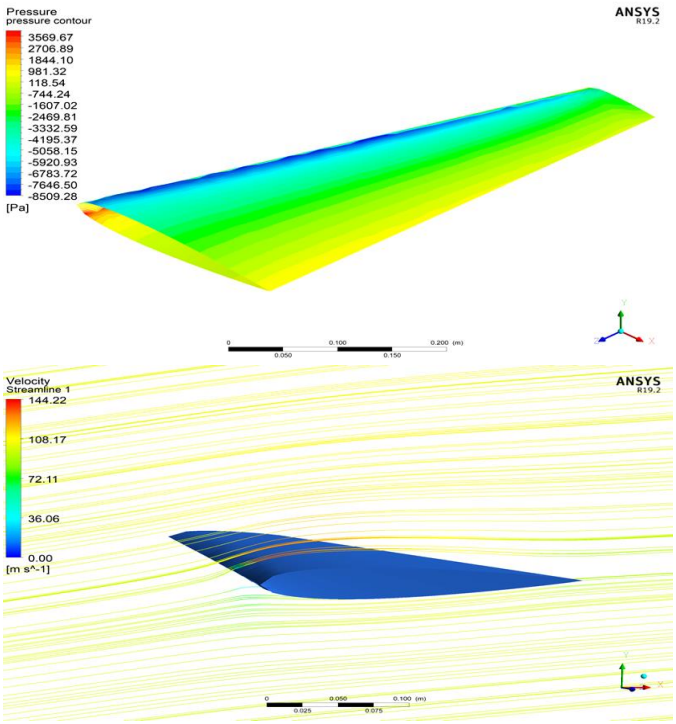

Fig. 16: Pressure distribution and velocity streamline contours for 8° angle of attack

0.66T

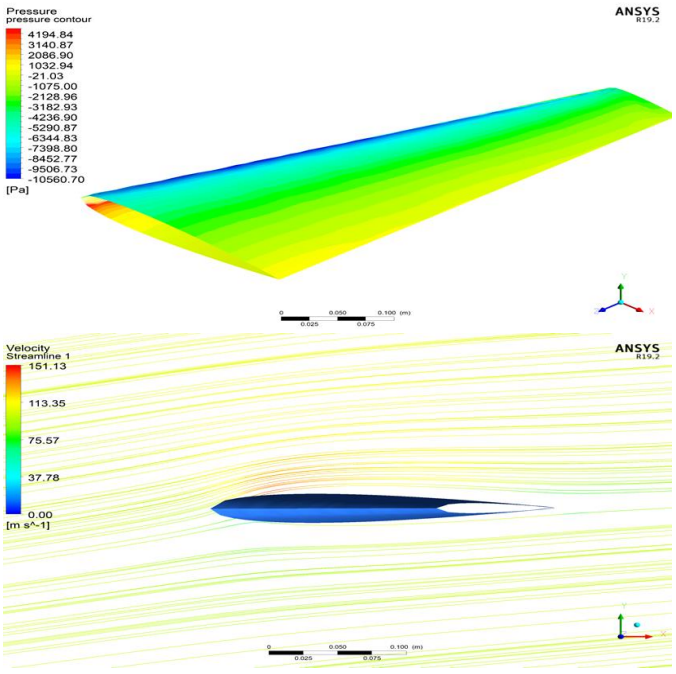

Fig. 17: Pressure distribution and velocity streamline contours for 10° angle of attack

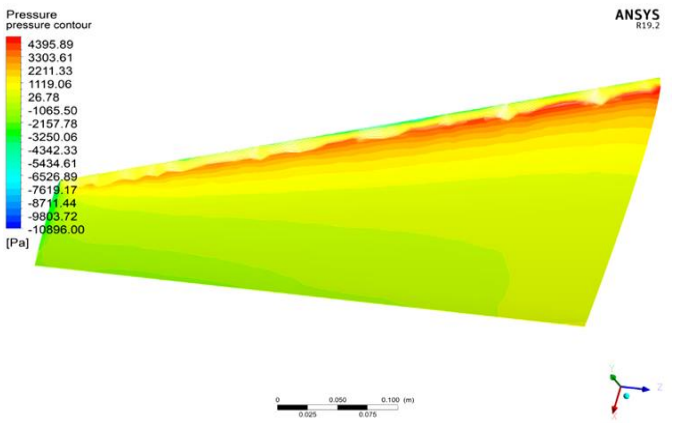

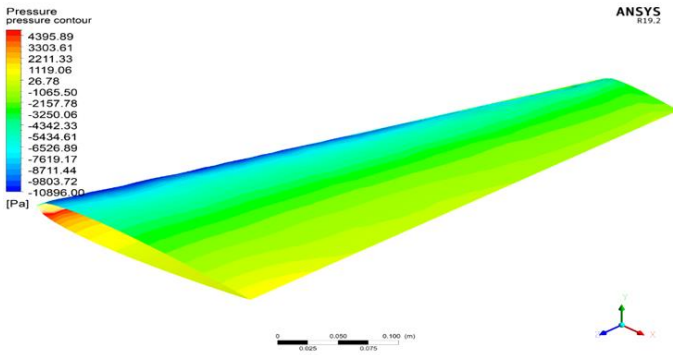

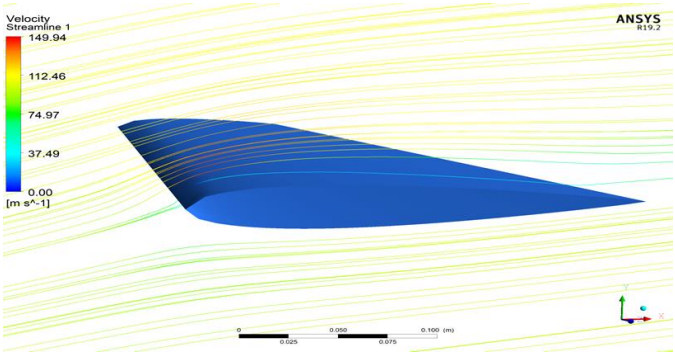

Fig.18: Pressure distribution and velocity streamline contours for 12° angle of attack

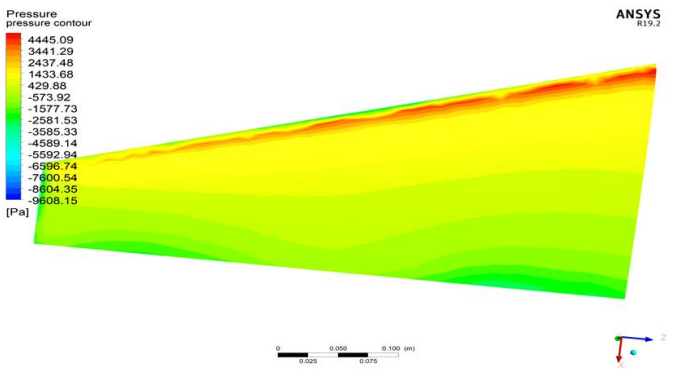

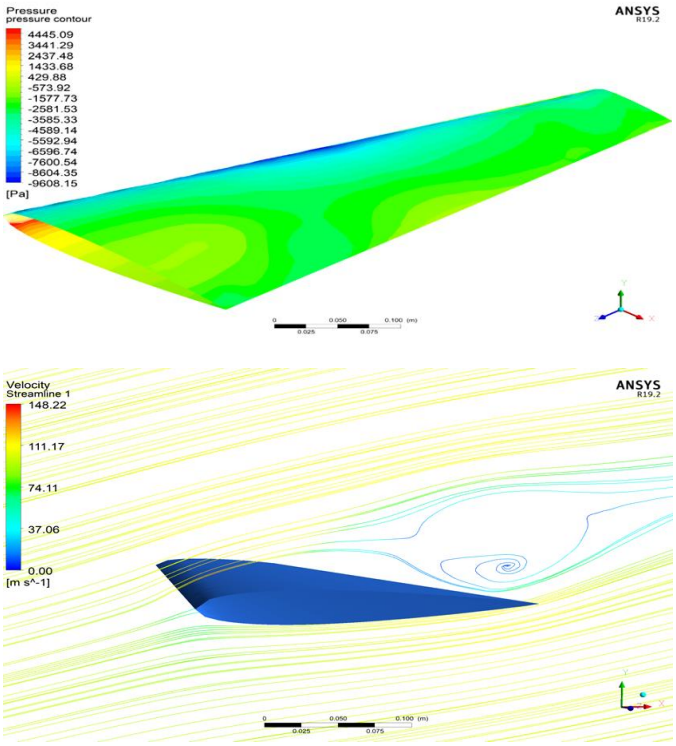

Fig. 19: Pressure distribution and velocity streamline contours for 14° angle of attack

5.2 Pressure and Velocity Streamline Contours for Wing with Winglet (90°):

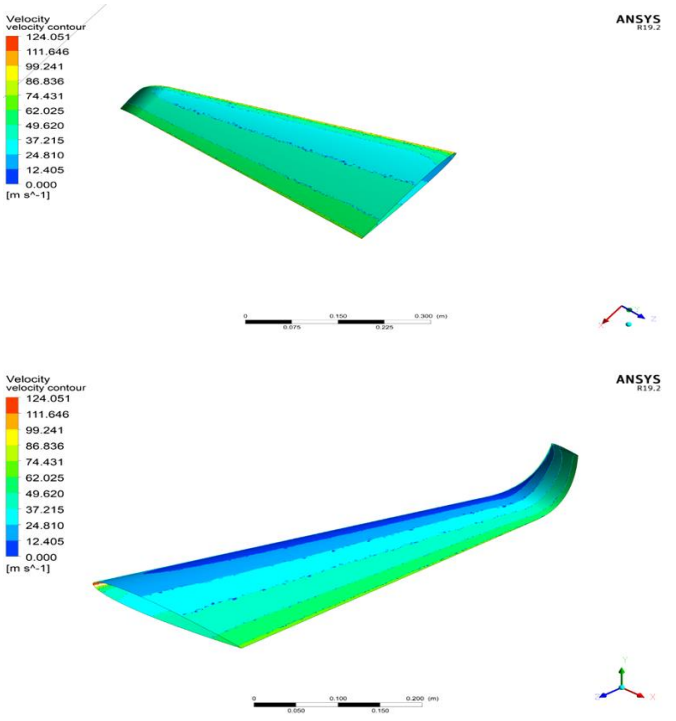

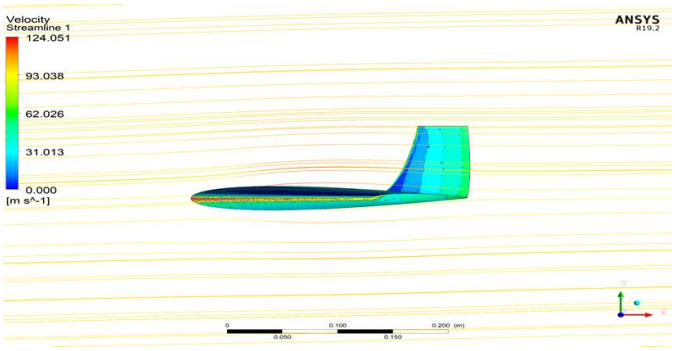

Fig. 20: Pressure distribution and velocity streamline contours for 2° angle of attack (winglet)

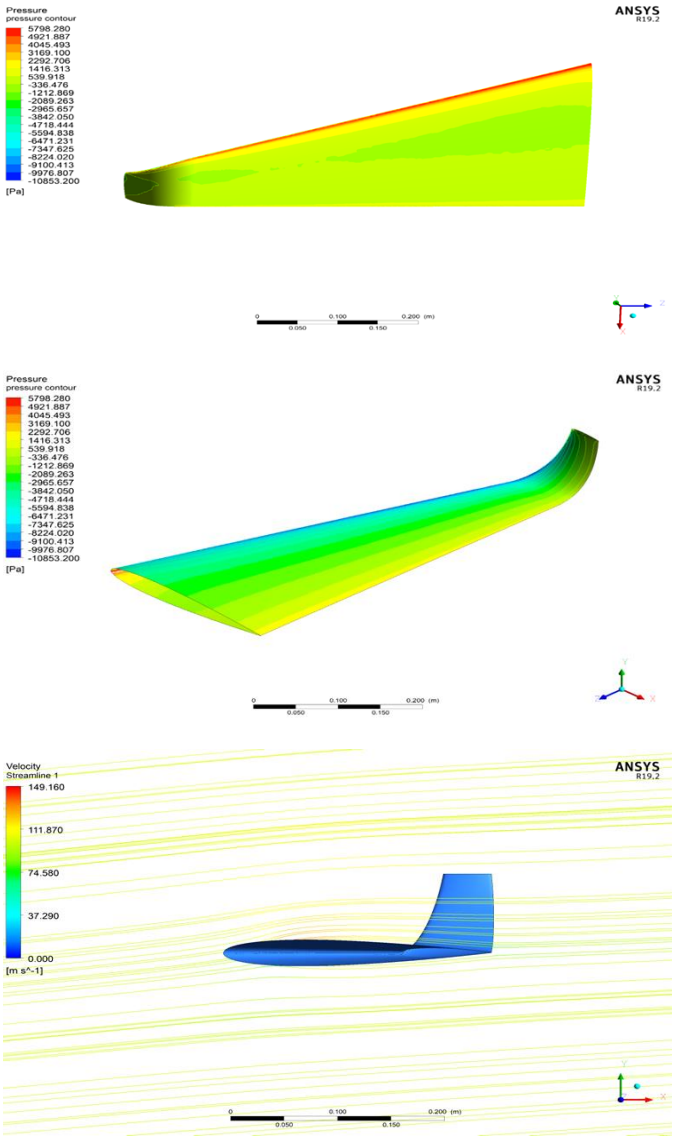

Fig. 21: Pressure distribution and velocity streamline contours for 6° angle of attack (winglet)

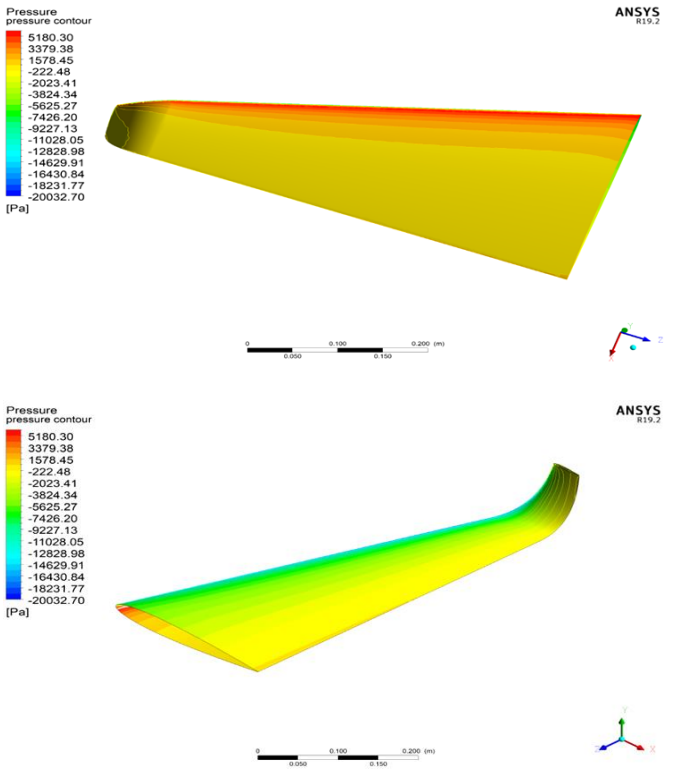

Fig. 22: Pressure distribution and velocity streamline contours for 10° angle of attack (winglet)

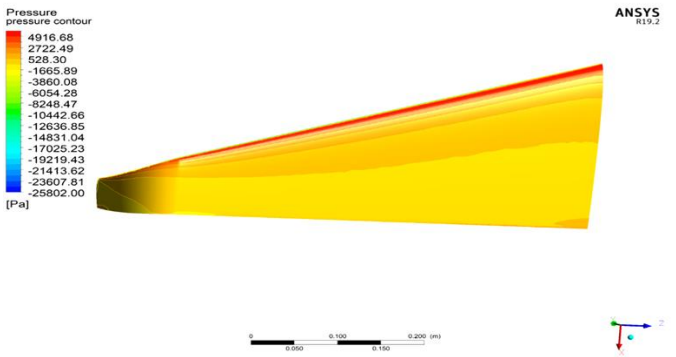

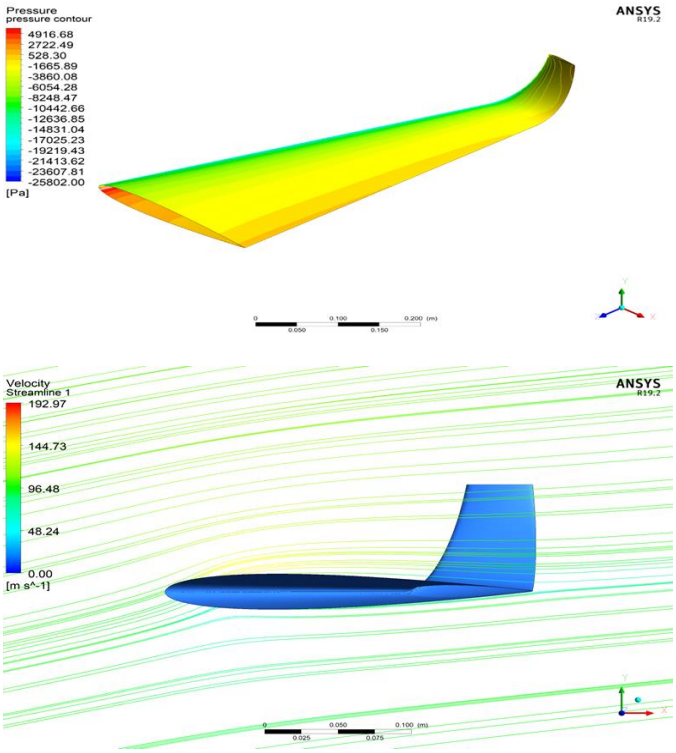

Fig. 23: Pressure distribution and velocity streamline contours for 12° angle of attack (winglet)

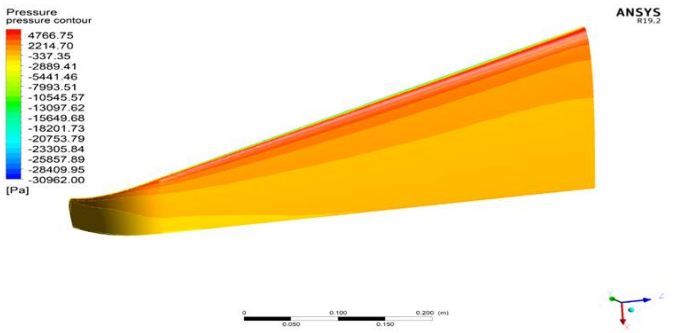

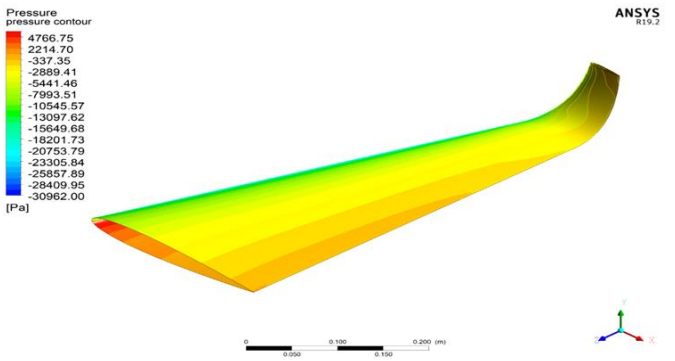

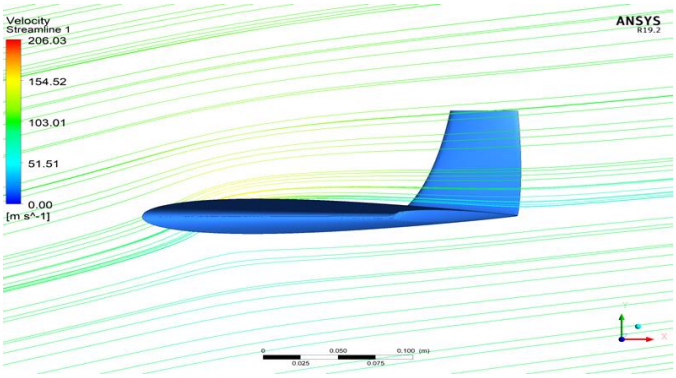

Fig. 24: Pressure distribution and velocity streamline contours for 14° angle of attack (winglet)

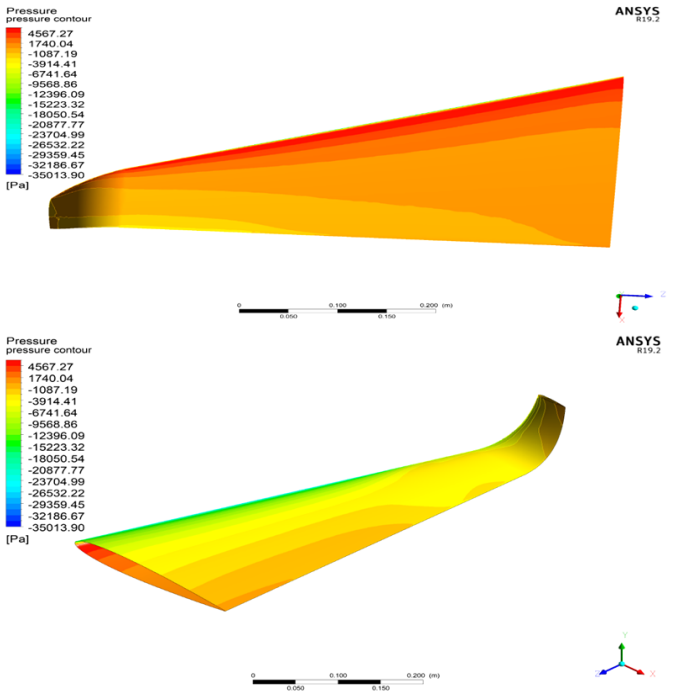

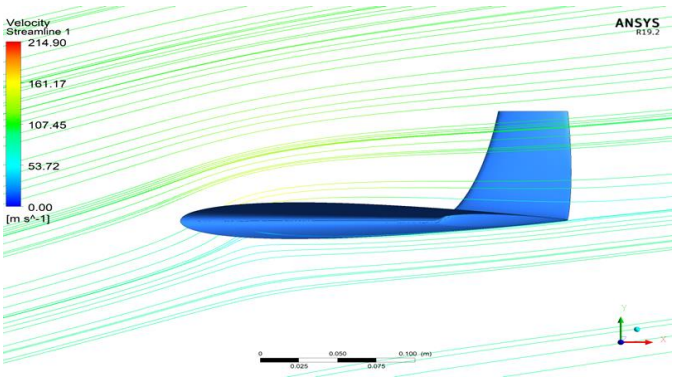

Fig. 25: Pressure distribution and velocity streamline contours for 16° angle of attack (winglet)

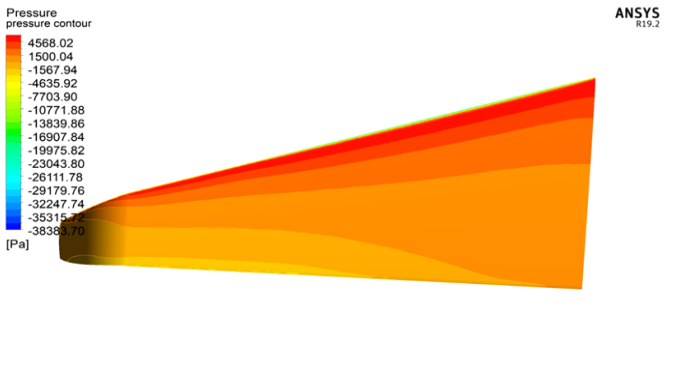

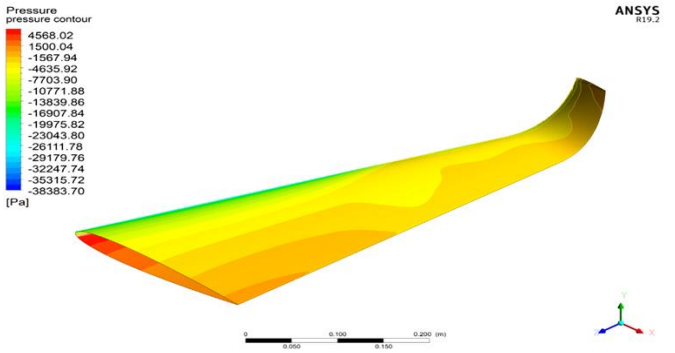

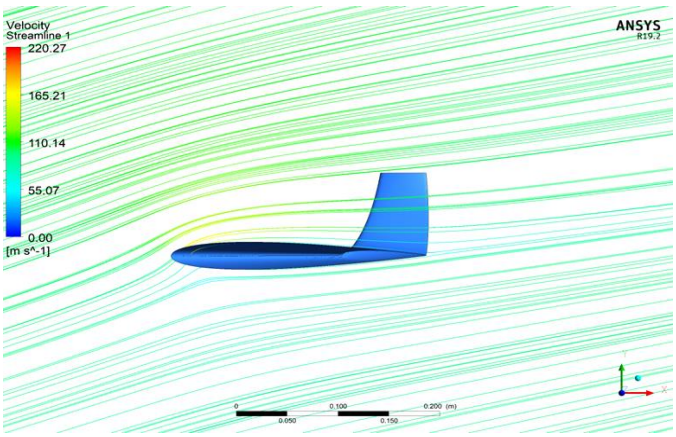

Fig. 26: Pressure distribution and velocity streamline contours for 18° angle of attack (winglet)

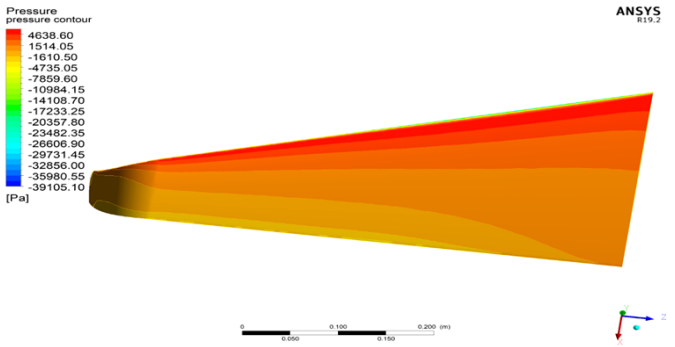

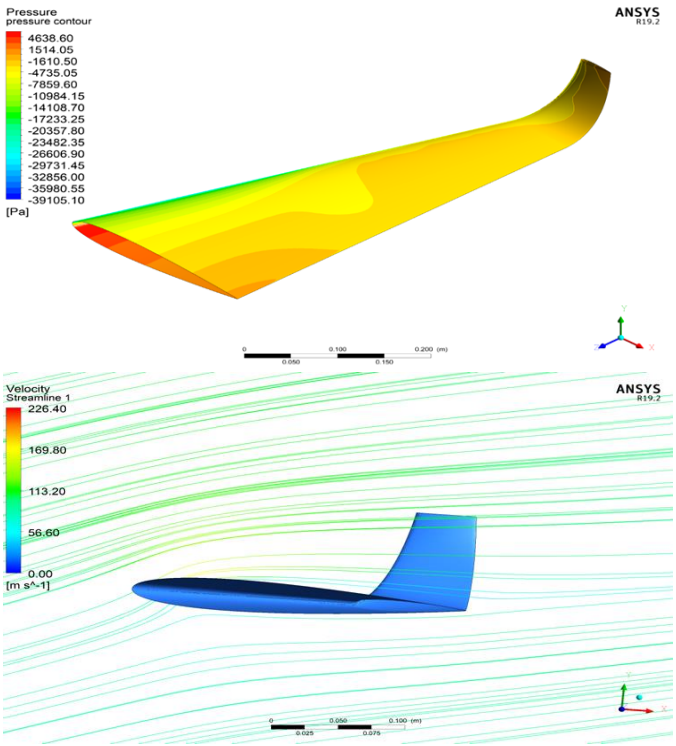

Fig. 27: Pressure distribution and velocity streamline contours for 20° angle of attack (winglet)

From figure. 13 to figure 27 where showing the pressure distribution contours of upper surface and lower surface of the wing, it can be observed that the pressure distribution at lower surface is increased at a higher rate with the increase of the value of incidence angle or angle of attack. For M_∞ = 0.3 which indicates the incompressible flow over the wing, there are assumed to be presence of no local supersonic flow occurred around the 3 dimensional wing. Also, it can be observed from the figures that the pressure distribution on the lower surface increased higher for wing with winglet than for normal wing. This ensures greater lift for wing with winglet as compared to for normal wing for the same value of angle of attack. Also at figure 13 to figure 27, the contours of velocity streamline has been shown for the observation of flow streamline which direction changes with the angle of attack. The feasible value of angle of attack at which stall of lift coefficient is discussed below which is required for the calculation of higher lift of the wing.

5.3 Pressure Coefficient (Cp) Vs. Position (X Co-ordinate):

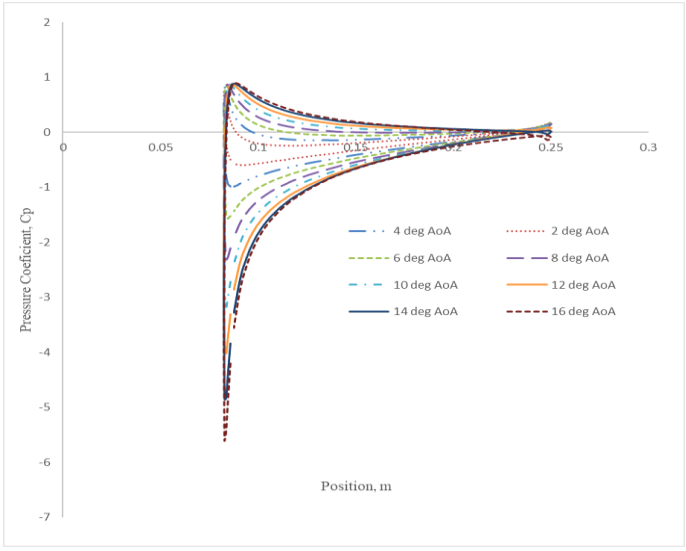

Fig. 28: Pressure Coefficient Vs. X coordinate position for wing with 90° winglet at mid span (z=250mm)

From above figure, it is evident that with the increase of angle of attack for same incompressible flow for wing with 90° winglet at mid span, the value of Cp at upper & lower wing surface increases which causes larger pressure difference between the upper and lower surfaces of the wing. From the above figure, it can be observed that for angle of attack 16°, Cp at upper surface will be larger at negative value causing largest pressure difference between the wing surfaces.

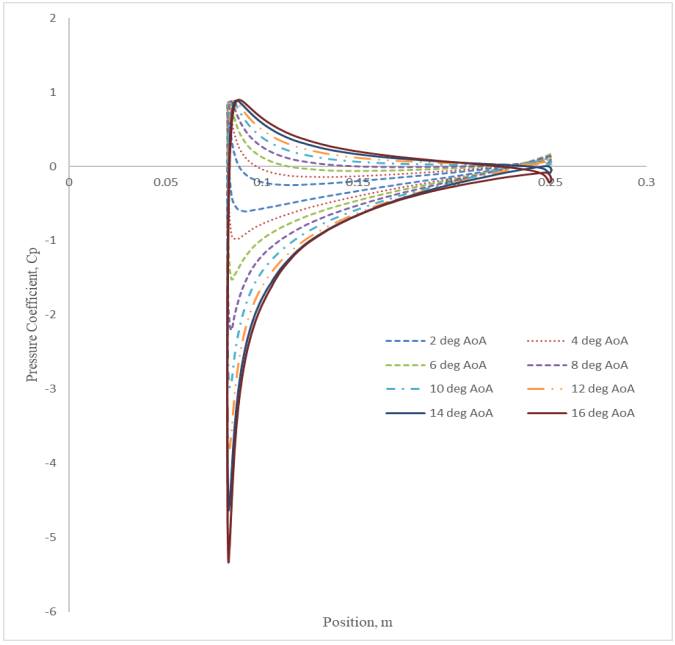

Fig. 29: Pressure Coefficient vs. X coordinate position for Wing with 30° winglet at midspan (z = 250mm)

From above figure, it can be observed that the values of Cp at upper and lower surfaces increases at both positive and negative sides with the increase of angle of attack. This causes comparatively larger pressure differences which causes larger lift and drag forces than before. From the above figure, the value of pressure coefficient at both ranges is greatest for 16° angle of attack.

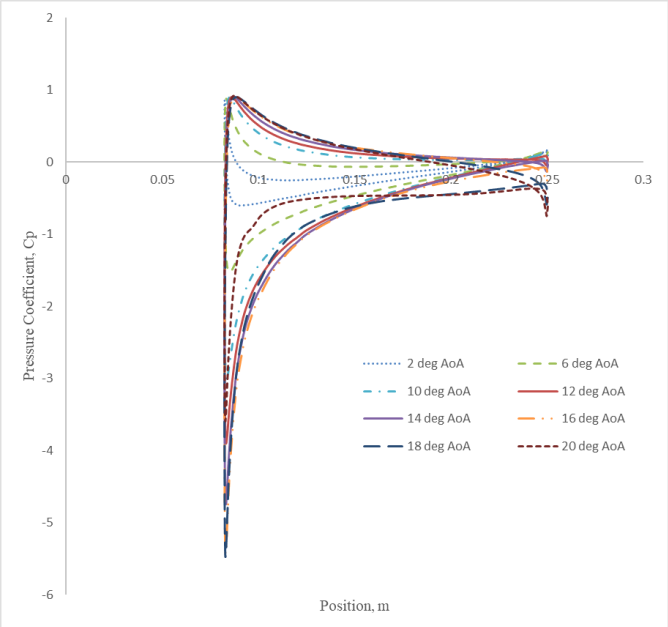

Fig. 30: Pressure Coefficient Vs. X coordinate position for Wing with 45° winglet at midspan (z = 250mm)

From above figure, it can be observed that the values of Cp at upper and lower surfaces increases at both positive and negative sides with the increase of angle of attack. This causes comparatively larger pressure differences which causes larger lift and drag forces than before. From the above figure, the value of pressure coefficient at both ranges is largest for 16° angle of attack. But for 20° angle of attack, the values of Cp at wing surfaces changes than before as stall of lift coefficient occurs. This figure indicates the Cp values improvements as the value of angle of attack changes incrementally.

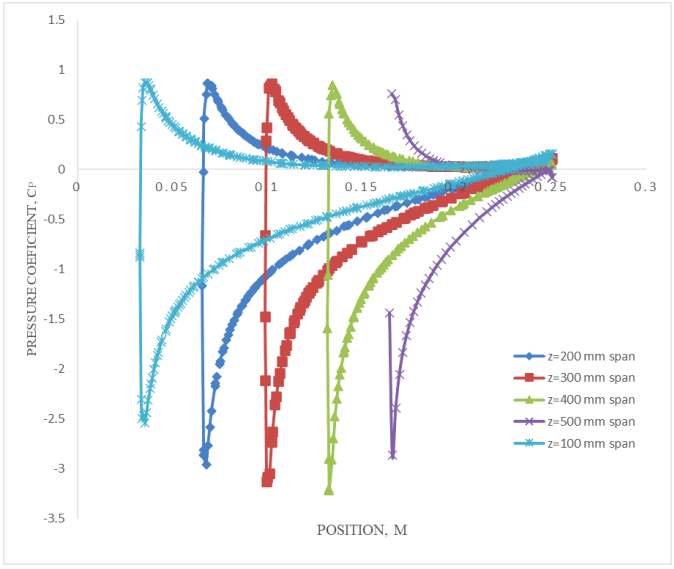

Fig. 31: Pressure coefficient Vs X coordinate position for different spanwise position for wing with 90° winglet at 10° AoA

This curve illustrates the pressure coefficients values vs. X coordinate positions at different chord section of the wing along Z-axis or spanwise direction for wing with 90° winglet for 10° AoA. Here, 5 iso-surfaces have been created forming 5 airfoils of NACA 0012 series of the 3 dimensional wing having different chord lengths. From the figure, it can be seen that the values for pressure coefficients at upper surface of the airfoils slightly increases at spanwise direction. At z = 400 mm, the value of Cp at upper surface is maximum but the value of Cp at lower surface remains constant along the spanwise direction. At z= 500 mm where the winglet is stalled, the Cp values again decreases as for reducing vorticity of flow due to the installment of winglet ensuring better values of lift coefficient.

5.4 Pressure Coefficient (Cp) Vs. Position (Y Co-ordinate):

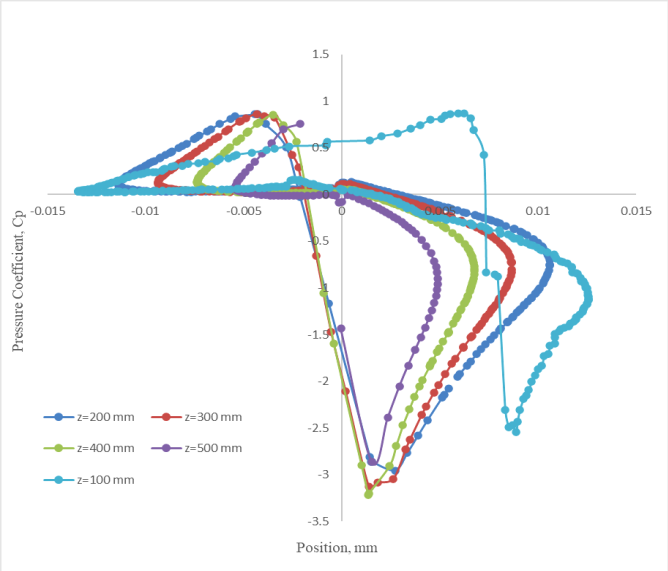

Fig. 32: Pressure coefficient Vs. Y coordinate positions for different spanwise position for wing with 90° winglet at 10° AoA

This figure illustrates the variation of Cp values vs. position at Y-coordinate at different spanwise chord sections for wing with 90° winglet at 10° AoA. It is evident that, the thickness of airfoils decreases with decreasing chord length along spanwise direction of the wing. From above figure, it is observed the ranges of Cp decreases as the span of the wing increases. So, it can be said that the pressure distribution gradually decreases along the thickness of the airfoils sections as the span of the wing increases. For z = 100 mm span, the ranges for Cp is maximum where the ranges of Cp is minimum at z= 500 mm where the winglet is stalled.

5.5 Lift Coefficients (C_L) and Drag Coefficients (C_D) for Normal Wing:

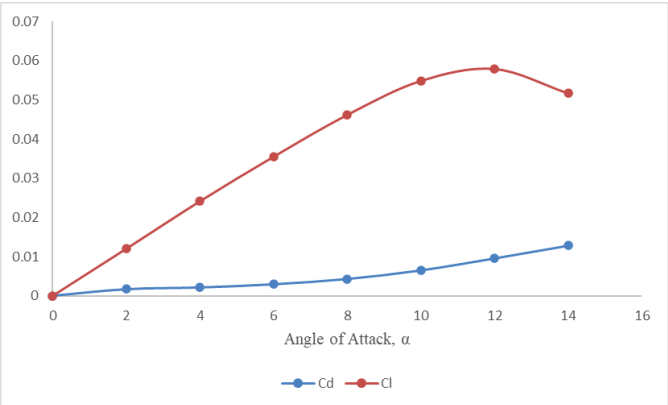

Fig. 33: C_L and C_D values Vs Angle of attack for Normal Wing

5.6 Lift Coefficients (C_L) and Drag Coefficients (C_D) for Wing with Winglets:

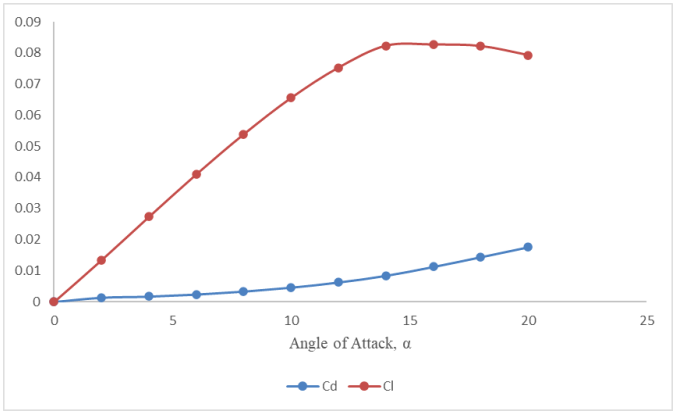

Fig. 34: C_L and C_D values Vs Angle of attack for Wing with 90° winglet

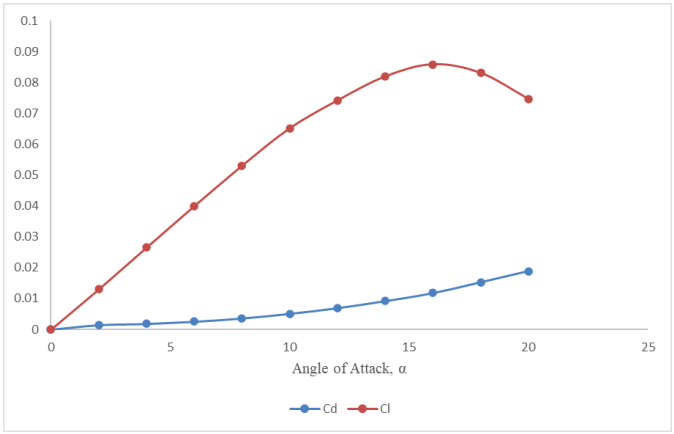

Fig. 35: C_L and C_D values Vs Angle of attack for Wing with 45° winglet

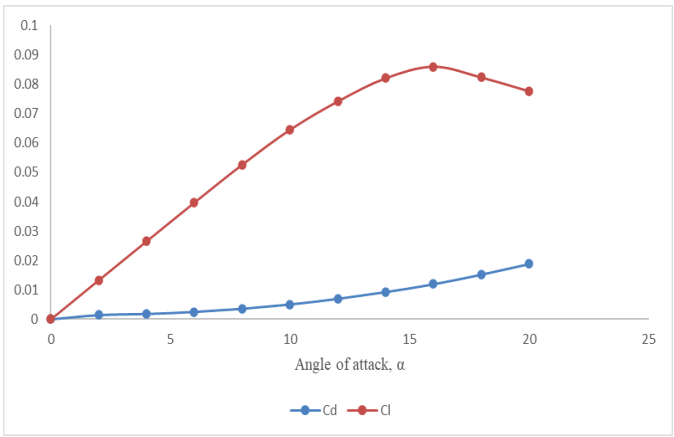

Fig. 36: C_L and C_D values Vs Angle of attack for Wing with 30° winglet

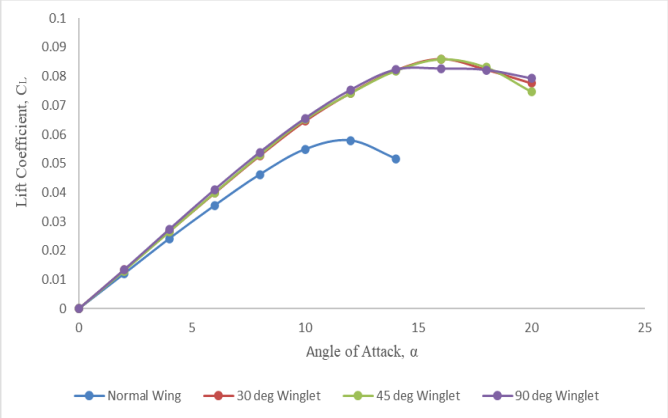

Fig. 37: C_L values comparison Vs Angle of Attack between Normal Wing and Wing with Winglets

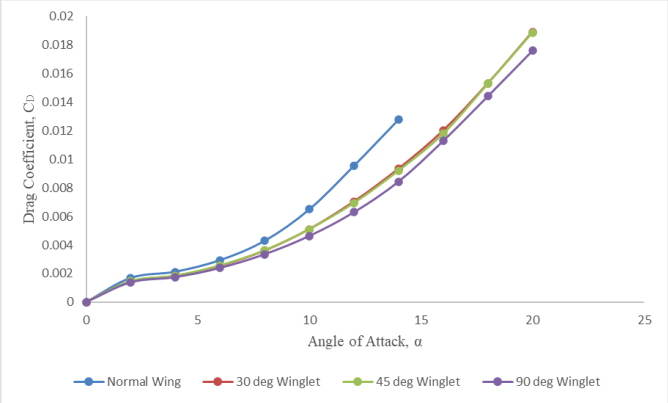

Fig. 38: C_D values Comparison Vs Angle of attack between Normal Wing and Wing with Winglets

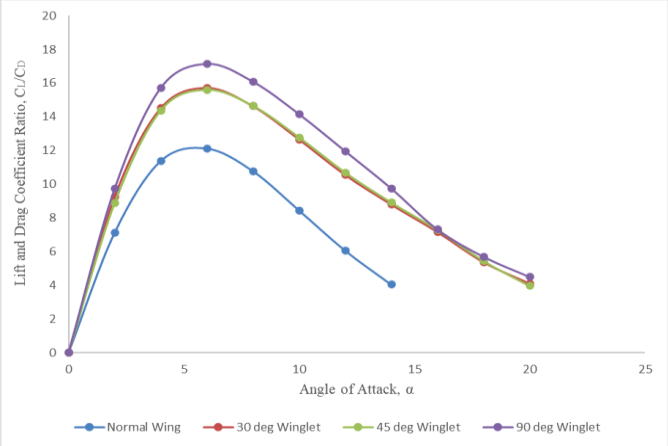

Fig. 39: C_L/C_D values Vs Angle of Attack between Normal Wing and Wing with Winglets

Above figures indicate the variations of lift and drag coefficients for normal wing, wing with 90° winglet, wing with 45° winglet and wing with 30° winglet. The values of CD exhibits smaller values as compared to lift coefficients. From these figure, the value of CL reaches a maximum peak point, CLmax ; corresponding to the related value of AoA. As the AoA values increases, the lift coefficient increases until stall occurs. The value of AoA at which stall of lift coefficient occurs is known as αstall. From fig. 34, it can be observed that for normal wing, the value of α stall is 12°. From fig. 35, the value of α stall for wing with is 14° AoA. From fig. 36 and fig. 37, the values of α stall is 16° for both wing with 45° winglet and wing with 30° winglet respectively. The drag coefficient values gradually increases with the increase of AoA values for all cases. As NACA 0012 series symmetric airfoil is used as cross section of all types of wing, so it is known that the zero lift of the wing will be at the zero angle of attack for the considered incompressible flow over the 3D wing. So here, $\alpha_{lift=0} = 0$.

The phenomenon of airfoil stall is of critical importance in airplane design. It is caused by flow separation on the upper surface of the airfoil. When separation occurs, the lift decreases drastically and the drag increases suddenly. Figure 4.25 shows the comparison of CL values among the types of wings. From the figure, CL values increases linearly with the increasing AoA when the flow attached relative to the wing. When the stall of airfoil at sections of wings occurred, stall of airfoils occurred. From figure 37, it can be seen that the maximum peak point value of CL,max is for wing for 30° winglet and 45° winglet around 0.085. The lift curves of wing for 90°, 30° and 45° winglet shows almost similar values with respect to the corresponding values of angle of attack. Figure 37 shows the greater values of CL of wing with winglets as compared to the normal wing which proves greater lift takes place if winglets are attached with normal wing. Winglets helps of reducing tip vortices at wing tip which causes higher values of CL. Fig. 38 shows the variation of CD values among the types of wings. From the figure, it is evident that the drag is reduced for wing with winglets as compared to normal wing. Drag line for wing with 90° winglet shows the lowest values of CD which is desired. As the values of AoA is increased, the values of CD is also increased both for normal wing and wing with winglets.

In fig. 39, the ratio of lift coefficient to drag coefficient values is represented with respected to the corresponding values of angle of attack. From the figure, it is observed that the lift to drag coefficient ratio exhibits maximum values for wing with 90° winglet. The values of CL/CD shows lowest values for normal wing. In the case of wing with 30° and 45° winglet, the values or curves seem similar with each other. So it can be said that the variations of results is negligible for wings with 30° and 45° winglets. For higher efficiency of aircraft engine and ensuring better fuel economy it is desired by improving lift force by increasing attached flow at wing tips reducing vorticity of free stream flow. Also it is desired that the drag force is as minimum as possible. From the above results and discussions, it is proved that the wing with 90°

winglet shows better results regarding the requirements of aerodynamics characteristics.

Table 4.1*(a)*: C_L and C_D values of 4 types of wings

SI No.	AoA α(°)	C_L (Normal Wing)	C_D (Normal wing)	C_L (90° winglet)
01	2	0.012	0.001688	0.0134
02	4	0.0241	0.002123	0.02732
03	6	0.0354	0.002932	0.040982
04	8	0.0461	0.0043	0.05385
05	10	0.0548	0.0065	0.0655
06	12	0.0578	0.00956	0.07525
07	14	0.0516	0.0128	0.0823
08	16	-	-	0.08261
09	18	-	-	0.08214
10	20	-	-	0.07924

Table 4.2*(b)*: C_L and C_D values of 4 types of wings

SI No	C_D (90° winglet)	C_L (45° winglet)	C_D (45° winglet)	C_L (30° winglet)	C_D (30° winglet)
01	0.00138	0.013	0.001465	0.01331	0.00144
02	0.001738	0.0265	0.001845	0.02655	0.00183
03	0.00239	0.03991	0.00256	0.03975	0.00253
04	0.003347	0.05297	0.00362	0.05266	0.0036
05	0.004626	0.065125	0.0051	0.06455	0.0051
06	0.006289	0.07413	0.0069386	0.0742	0.007
07	0.008436	0.0819	0.0092	0.08208	0.009
08	0.011286	0.08586	0.01178	0.086	0.012
09	0.014413	0.0831	0.01528	0.08231	0.0153
10	0.0176	0.0747	0.01886	0.07762	0.0189

From the above table, for normal wing at αstall, CL = 0.0578

And for wing with 90° winglet at αstall, CL = 0.08214

Therefore, percentage of increased lift by using 90° winglet, $= \frac{(0.08214-0.0578)}{0.0578} = 0.4211$

= 42.11%

For wing with 45° winglet at αstall, CL,max = 0.08586

Therefore, percentage of increased lift by using 45° winglet, $= \frac{(0.08586-0.0578)}{0.0578} = 0.4855$

= 48.55%

For wing with 30° winglet at αstall, CL,max = 0.086

Therefore, percentage of increased lift by using 30° winglet, $= \frac{(0.086-0.0578)}{0.0578} = 0.487889$

= 48.79%

So, considering the improvement of lift coefficient, usage of 30° winglet shows most lift coefficient increment. But also as compared to reduced drag coefficient, wing with 90° winglet shows better performance.

6. CONCLUSION

6.1 Conclusion:

This study involves with numerical analysis of the performance of aerodynamics characteristics of aeroplane wing with and without winglets. The present work shows that winglets are one of the important device to achieve better aerodynamic performance of the aircraft.

This work proposes alternatives in the cant angles of the winglets from the conventional wing without winglets. An improved winglet design with at a certain cant angle will significantly yield a better performance of an aircraft by lowering the induced drag which causes tip vortices. The overall improved aerodynamic efficiency will result in reduced fuel consumption.

Results clearly shown that using blended winglet lift coefficient is increased approximately 42% to 49% and drag coefficient is reduced.

This winglet designs are capable of to reduce induced drag force and convert wing tip vortices to additional thrust which will save cost by reducing the usage of fuel, noise level reduction and increase the efficiency of the aircraft engine.

6.2 Future scopes of the work:

The analysis can be done experimentally constructing a model of normal wing and wing without winglets and then a comparison can be established between the variations of the result.

The work can be extended for different Reynolds number and flow types of free stream to investigate the lift and drag coefficients with respect to the types of flow accordingly.

The analysis can be done for asymmetric airfoil sections wings to investigate whether it shows better aerodynamic results than before or not.

The work can be extended for a larger range of angle of attack and also for different viscous models.

ACKNOWLEDGEMENT

We would like to thank Almighty Allah for His kindness upon us without which it would be impossible to finish this paper. We would like to pay our sincere gratitude to Dr. Abdullah Al-Faruk, Professor, Department of Mechanical Engineering, Khulna University of Engineering & Technology (KUET) for his guidance, support and concern throughout this paper. We are indebted to him. We express our cordial gratefulness to Dr. Mohammad Ariful Islam, Professor Department of Mechanical Engineering, Khulna University of Engineering & Technology (KUET), for providing a great opportunity to enhance presentation and study based skills which will later help flourishing in different sectors. We also highly appreciate the lab facilities we got from CUET.

REFERENCES

[1] F. Culick, ""The Wright Brothers: First Aeronautical Engineers and Test Pilots"," AIAA Journal, vol. 41, pp. 985-1006, 2003.

[2] R. Whitcomb, ""A Design Approach & Selected Wind Tunnel Results at High Subsonic Speeds for Wing-Tip Mounted Winglets"," NASA TN D-8260, June 1976.

[3] P. Bourdin, A. Gatto and M. Friswell, ""Aircraft Control Via Variable Cant-Angle Winglets"," Journal of Aircraft, vol. 45, March-April 2008.

[4] E. Houghton and P. Carpenter, Aerodynamics for Engineering Students, 4th ed., Edward Arnold Publisher.

[5] J.-J. Chattot, ""Analysis and Design of Wings and Wing/Winglet Combinations at Low Speeds"," 42nd AIAA Aerospace Sciences Meeting and Exhibit, 5-8 January 2004.

[6] P. D. Gall and H. C. Smith, ""Aerodynamic Characteristics of Biplanes with Winglets"," Journal of Aircraft, vol. 24, no. 8.

[7] I. Kroo, J. McMasters and S. C. Smith, ""Highly Nonplanar Lifting Systems, Presented at: Transportation Beyond 2000: Technologies Needed for Engineering Design"," NASA Langley Research Center, 26-28 September 1995.

[8] M. Smith, N. Komerath, R. Ames, O. Wong and J. Pearson, ""Performance analysis of a wing with multiple winglets"," AIAA Applied Aerodynamics, 2001.

[9] J. Spillman and M. McVitie, ""Wing tip Sails which give lower drag at all normal flight speeds"," Aeronautical Journal, vol. 88, pp. 362-369, 1984.

[10] A. Hossain, A. Rahman, A. P. Iqbal, M. Ariffin and M. Mazian, ""Drag Analysis of an Aircraft Wing Model with and without Bird Feather like Winglet"," International Journal of Science, Engineering and Technology, vol. 5, no. 9, 2011.

[11] A. Beechook and J. Wang, ""Aerodynamic Analysis of Variable Cant Angle Winglets for Improved Aircraft Performance"," 19th International Conference on Automation & Computing, pp. 13-14, September 2013.

[12] C. R. and F. Catalano, ""Aerodynamic Analysis of Multi Winglets for Low Speed Aircrafts"," 27th International Congress of Aeronautical Sciences.

[13] B. S. .. Mattos, A. P. Macedo and D. H. d. S. Filho, ""Considerations about Winglet Design"," 21st Applied Aerodynamic Conference, AIAA 2003-3502, 23-26 June 2003.

[14] N. J. Pfeiffer, ""Numerical Winglet Optimization"," "42nd AIAA Aerospace Sciences Meeting and Exhibit", 5-8 January 2004.

[15] J. Himisch, ""Winglet Shape and Load Optimization with a numerically supported Lifting Line Method"," 12th AIAA/ISSMO Multidisciplinary Analysis and Optimization Conference, 10-12 September 2008.

[16] D. Mylisamy and P. P. S, ""Performance Investigation of an Aircraft Wing at Various Cant Angles of Winglets using CFD Simulation"," July 2015.

[17] J. D. Anderson, "Fundamentals of Aerodynamics", 5th ed., McGraw Hill Education Private Limited Publication.

[18] [Online]. Available: https://www.researchgate.net/figure/The-Development-of-Wingtip-Vortices-Scott-2005_fig1_284027599.

[19] [Online]. Available: http://www.airfoiltools.com/plotter/index.

BIOGRAPHIES

Md. Shahadat Hossan Sayem, graduate student in the department of Mechanical Engineering from Khulna University Of Engineering & Technology, (KUET), Khulna, Bangladesh.

Md. Mainuddin Sagar, graduate student in the department of Mechanical Engineering from Chittagong University Of Engineering & Technology, (CUET), Chittagong, Bangladesh.

Md. Rezwan Alam, graduate student in the department of Mechanical Engineering from Khulna University Of Engineering & Technology, (KUET), Khulna, Bangladesh.

Dr. Abdullah Al- Faruk, Professor in the department of Mechanical Engineering from Khulna University Of Engineering & Technology, (KUET), Khulna, Bangladesh.